Universidade de São Paulo
Instituto de Astronomia, Geofísica e Ciências Atmosféricas
Departamento de Astronomia

Danilo Couto de Souza

Cyclones in Southwestern Atlantic: Life Cycle and Energetics

São Paulo

2024

Danilo Couto de Souza

Cyclones in Southwestern Atlantic: Life Cycle and Energetics

Tese apresentada ao Programa de Meteorologia do Instituto de Astronomia, Geofísica e Ciências Atmosféricas da Universidade de São Paulo como requisito parcial para a obtenção do título de Doutor em Ciências.

Área de Concentração: Meteorologia

Orientador: Prof. Dr. Pedro Leite da Silva Dias

Coorientador: Prof. Dr. Ricardo de Camargo

São Paulo

2024

O que há de melhor tá na vida, na transformação da natureza.

Acknowledgements

- Mulher;
- Família;
- Orientadores Pedro Dias e Ricardo de Camargo
- Ex-orientadores: Renato Ramos da Silva, Roberto Carelli Fontes e John Beardall;
- Pesquisadores e professores: Carolina Gramcianinov, Pedro Peixoto, Felipe Bragança Alves;
- Colegas: Matheus Bonjour, Renan Godoy, Maria Luiza Kovalski, e toda equipe do MASTER;
- Suporte técnico: Jean Peres, Djalma, Sebastião e Samuca;
- LNCC: rodadas com SDumont;
- Alexandra Elbakyan, Aaron Swartz e toda comunidade *open source*

Esta tese/dissertação foi escrita em LaTeX com a classe IAGTESE, para teses e dissertações do IAG.

“一、努力の精神を養うこと”

“*First, foster the spirit of effort*”

“*Primeiro, criar o intuito do esforço*”

Kanga Sakukawa

Resumo

Resumo

Abstract

Abstract

List of Figures

List of Tables

Contents

Chapter 1

Introduction

1.1 *Objetivo e pergunta de pesquisa*

- Como a interação oceano-atmosfera afeta a energética de sistemas ciclônicos no Atlântico Sul?

1.2 *Objetivos específicos*

- Determinar padrões, através do Ciclo Energético de Lorenz, para os ciclones atuantes no Atlântico Sul dentre o período 1979-2020;
- Avaliar qual o conjunto de parametrizações microfísicas e de convecção propiciam que o modelo MPAS-A apresente simulações mais realistas do Furacão Catarina, em diferentes estágios de desenvolvimento do sistema;
- Determinar o impacto das diferentes configurações do modelo na energética do sistema;
- Avaliar o impacto da pertubação da temperatura da superfície do mar na energética de sistemas ciclônicos atuantes no Atlântico Sul, através do estudo de casos representativos.

Chapter 2

Theoretical Background

2.1 Cyclones: Categories and Definitions

For an effective analysis and study, a phenomenon must first be accurately defined. The Glossary of Meteorology by American Meteorological Society (2012) characterizes a "cyclone"as "An atmospheric cyclonic circulation, a closed circulation. A cyclone's direction of rotation (counterclockwise in the Northern Hemisphere) is opposite to that of an anticyclone. (...) Because cyclonic circulation and relative low atmospheric pressure usually coexist, in common practice the terms cyclone and low are used interchangeably. Also, because cyclones are nearly always accompanied by inclement (often destructive) weather, they are frequently referred to simply as storms". This definition categorizes cyclones into sub-types based on their occurrence location: tropical, extratropical, and subtropical cyclones (Reboita et al., 2017, e.g.). This classification is supported by the assumption that cyclones within the same latitude bands share genesis environments and dynamic maintenance processes. There are also cyclones whose genesis is found in high latitudes, called polar lows (Emanuel and Rotunno, 1989; Harrold and Browning, 1969, e.g.). These will not be discussed in depth as the focus of the present study is on the systems generated in the adjacent regions to the South American coast.

The aforementioned definition, while broad, lacks precise criteria. Thus, subsequent sections will employ the Aristotelian approach to elucidate physical phenomena (Aristotle and Aristotle, 1933). Aristotelian causes, foundational to Aristotle's philosophy, offer a comprehensive explanation for an object or phenomenon's existence through four types: material, formal, efficient, and final causes. The ensuing subsections will detail each cause, enhancing the understanding of related phenomena. For each cyclone type — extratropical and tropical — a discussion of the causes will facilitate a direct comparison between the systems.

It is important to note that the structure and mechanisms underlying the genesis and development of cyclones have been well-documented since the mid-twentieth century, leading to the inclusion of many historical references. The aim is to highlight distinctions between cyclone types, a comparison not commonly made in literature. Meteorologists often specialize as "tropical meteorologists" or "mid-latitude meteorologists", a division reflected in educational materials. Some texts focus exclusively on mid-latitude or tropical dynamics (Chan and Kepert, 2010; Bluestein, 1992, e.g.), while others that address both, treat them separately (Holton, 1973; Donald Ahrens and Henson, 2015, e.g.). Although this separation is customary and beneficial, juxtaposing the two offers novel insights, as explored in the following sections.

2.1.1 Material Causes

Material cause, within the Aristotelian framework, denotes the substance or constituents that form an object. It encompasses the matter or physical elements constituting an entity, serving as the foundation for its existence. For instance, wood acts as the material cause for a table, just as water serves as the material cause for a river. Applied to cyclonic systems, the material cause encompasses the air masses forming these systems, particularly emphasizing their thermal structure. This section elaborates on this concept, showcasing its relevance in defining and categorizing cyclonic systems.

The concept of an air mass, as introduced by Swedish meteorologist Tor Bergeron in 1928, describes a large body of air characterized by uniform temperature, moisture, and other properties, extending over 500 to 5000 km and encompassing the troposphere's full height (Stull, 2015). Air masses are classified based on their temperature, moisture content, stratification, and turbidity levels. Additionally, air masses originate from specific source regions, areas conducive to their formation. The characteristics of an air mass are significantly influenced by its source region's surface conditions, necessitating a flat terrain and mild winds for its development (Donald Ahrens and Henson, 2015). Heat transfer between the surface and the air is gradual, requiring the air mass to remain over its source region for an extended period to assimilate its properties (Spiridonov and Ćurić, 2021). Therefore, mid-latitudes, characterized by variable meteorological conditions and strong winds, are generally unsuitable for air mass formation.

Bergeron's classification system is the most widely accepted methodology for categorizing air masses. It utilizes letters to denote the moisture content and the origin of air masses (Spiridonov and Ćurić, 2021). The initial letter signifies the air mass's moisture source—continental (dry) or maritime (moist)—while the subsequent letter indicates the geographical origin of the air mass, whether it be tropical (T), polar (P), arctic/antarctic (A), equatorial (E), or monsoonal (M). Figure 2.1 illustrates the spatial distribution of air masses according to Bergeron's scheme. Upon the encounter of two distinct air masses, immediate mixing does not occur, resulting in a temporary discontinuity at their intersection, known as fronts (Spiridonov and Ćurić, 2021; Donald Ahrens and Henson, 2015).

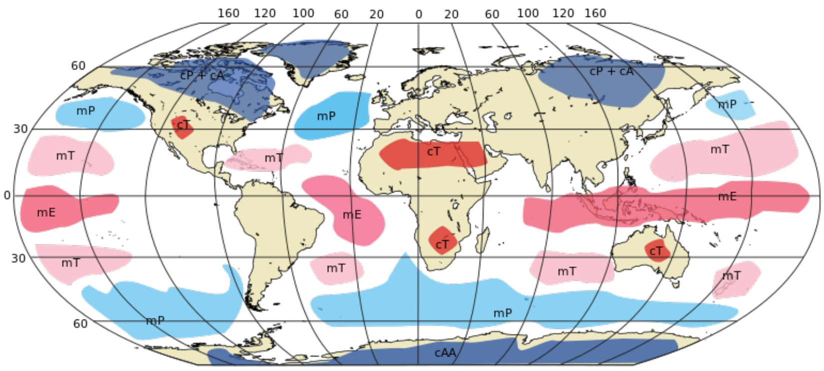

Figure 2.1: Spatial distribution of air masses according to Bergeron's classification. Credit: public domain (https://commons.wikimedia.org/w/index.php?curid=12526643).

Therefore, the validity of the traditional cyclone classification—tropical, extratropical, and subtropical—relies on the premise that different types of cyclones are initiated by distinct air masses. Specifically, tropical cyclones originate from warm, moist air masses that span the entire troposphere and form over warm tropical waters (Gray, 1968; Frank, 1977a; Ramage, 1959; Riehl, 1948). In contrast, extratropical cyclones are associated with frontal zones at mid-latitudes, where two different air masses meet, and are typically linked to cold cores (Bjerknes and Holmboe, 1944; Shapiro and Keyser, 1990; Hart, 2003). However, intense marine extratropical cyclones can experience warm seclusion, resulting in a warm core at the system's center (Hart, 2003; Shapiro and Keyser, 1990). Subtropical cyclones feature a hybrid structure between tropical and extratropical systems, with warm, moist cores that are less pronounced and shallower than those in tropical cyclones (Hart, 2003).

Hart (2003) offers an objective methodology for identifying the thermal structure of cyclonic systems. This analysis focuses solely on tropospheric levels (up to 300 hPa) because cyclones display an opposing thermal signal in the stratosphere. The study examines layers between 900 and 600 hPa and between 600 and 300 hPa, which have comparable masses. Levels below 900 hPa are excluded to prevent extrapolation below the ground or into the boundary layer, which may not accurately represent the cyclone's structure in the free atmosphere. Consequently, the variable corresponding to the cyclonic perturbation in height is defined as follows:

$$\Delta Z = Z_{MAX} - Z_{MIN} \tag{2.1}$$

Where Z_{MAX} and Z_{MIN} represent the maximum and minimum geopotential heights at a specific isobaric level, measured within a 500 km radius from the cyclone's center. Following this definition:

$$\Delta Z = \frac{dg|V_g|}{f} \tag{2.2}$$

Here, d denotes the distance between the geopotential height extremes, g is the acceleration due to gravity, f represents the Coriolis parameter, and V_g is the geostrophic wind speed. Consequently, the cyclone's vertical structure (indicative of a cold or warm core) is determined by the vertical gradient of ΔZ, which is proportional to the magnitude of the scaled thermal wind (V_T) for a constant d, applied across two tropospheric layers of equal mass:

$$\left.\frac{\partial(\Delta Z)}{\partial \ln p}\right|_{600hPa}^{300hPa} = -|V_T^U| \tag{2.3}$$

$$\left.\frac{\partial(\Delta Z)}{\partial \ln p}\right|_{900hPa}^{600hPa} = -|V_T^L| \tag{2.4}$$

where V_T^U and V_T^L symbolize the thermal winds at upper and lower levels, respectively. As such, positive values of $-V_T$ signify a warm core within the respective layer, whereas negative values indicate a cold core.

The relationship between the temperature and depth of the core within cyclonic systems is detailed through a phase diagram by Hart (2003), depicted in Figure 2.2. This diagram utilizes the abscissas to represent the parameter $-V_T^L$, illustrating the low-level core's thermal structure. The ordinates display $-V_T^U$, portraying the high-level core's thermal structure. Integrating these metrics allows for discerning whether a system possesses a warm or cold core, and if it is shallow or deep. Figure 2.2 includes typical positions representative of different cyclonic types within the phase space. As noted by Hart (2003), a system may shift within this diagram throughout its lifecycle, making the depiction general for each cyclone category. Additionally, Hart proposes a diagram for the horizontal structure of these systems, related to their formal causes, which is addressed in Section 2.1.2.

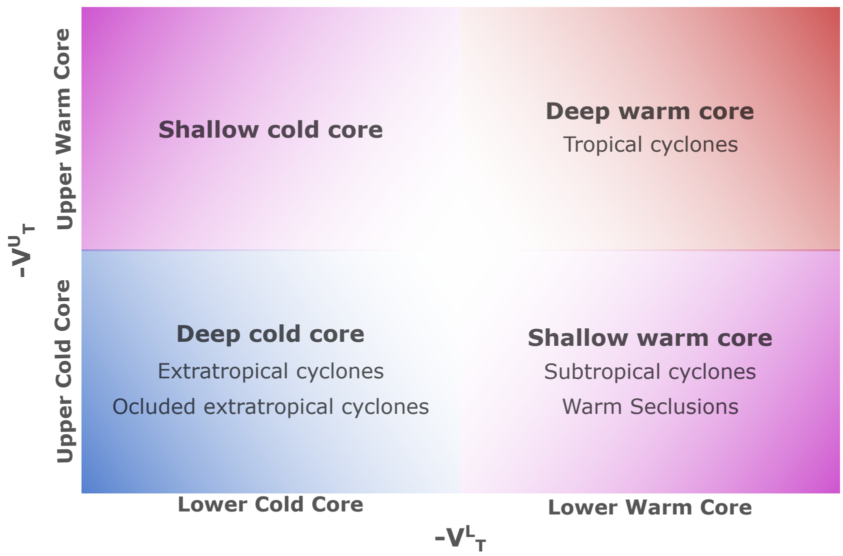

Figure 2.2: Phase diagram showing the relationship between the core temperature of cyclonic systems and their classification. Adapted from Hart (2003).

Thus, material causes, tied to the thermal structure of cyclonic systems, offer a foundational method for classifying and differentiating cyclone types. This classification leverages the phase diagram by Hart (2003) for an objective categorization. Accordingly, extratropical cyclones are characterized by cold, deep cores, whereas tropical cyclones feature warm, deep cores. This spectrum isn't binary; there exists a gradient of thermal structures with systems exhibiting intermediate features classified as subtropical cyclones. Nevertheless, relying solely on thermal attributes for classification is insufficient. For instance, extratropical cyclones, through the warm seclusion process (Shapiro and Keyser, 1990, e.g.), can develop warm, shallow cores (Hart, 2003), indicating the necessity for a broader analysis incorporating additional Aristotelian causes for a comprehensive classification.

2.1.2 Formal Causes

The formal cause concerns the essence or identity that defines a thing, essentially its design, structure, or conceptual blueprint that marks it as a particular type. To revisit the earlier example of a table from Section 2.1.1, its formal cause is the design that qualifies it as a table rather than a chair. In the context of cyclones, the formal cause refers to the system's organizational structure, such as the configuration of convection bands and/or fronts, along with the low-pressure pattern.

Extratropical cyclones, typically associated with mid-latitudes and frontal structures, exhibit an average diameter between 1200 and 1800 km. This size fluctuates over their lifecycle, with the cyclone's diameter expanding by up to 150% during its intensification phase (Simmonds, 2000; Rudeva and Gulev, 2007). However, the spatial complexity and variability of these systems throughout their lifecycle pose methodological challenges for accurately estimating their dimensions and comparing findings across different studies.

The seminal model describing the formation and horizontal structure of extratropical cyclones was introduced by Bjerknes (1919), illustrated in Figure 2.3. This model showcases the cyclone's movement along a central horizontal line, with the "steer line"demarcating the boundary that influences the cyclone's trajectory, characterized by warm air masses to its left. The "squall line"indicates a zone of intense meteorological activity, marked by strong winds and often heavy precipitation, with cold air masses located to its left. The "fore runner"represents a region of diverging airflow.

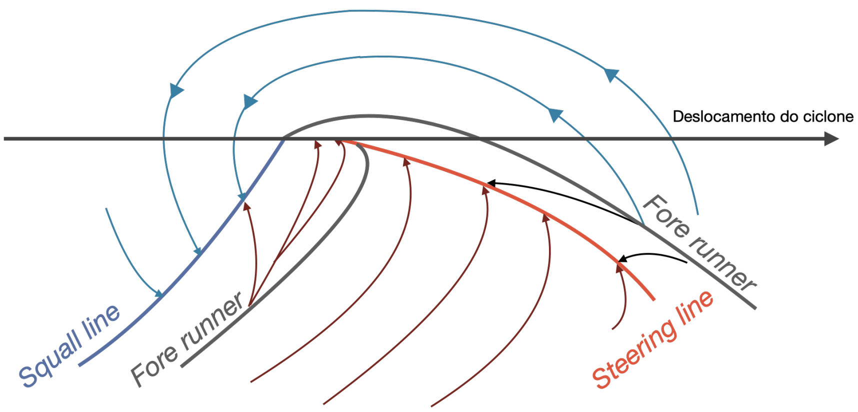

Figure 2.3: Representation of the Bjerknes model for the extratropical cyclone formation process and its horizontal structure. Cold air regions are illustrated with blue lines, while warm air regions with red lines. Adapted from Bjerknes (1919).

Bjerknes and Solberg (1922) realized that the model proposed in Bjerknes (1919) represented just one phase in the life cycle of cyclones, indicating that there are several stages of development. Bjerknes and Solberg (1922) established the Polar Front Theory, which is the foundation of the so-called Norwegian cyclone model. Schultz et al. (1998) synthesizes and describes the development of extratropical cyclones according to this theory, so that a visual representation of the horizontal structure at the surface during different stages of cyclone evolution is found in Figure 2.4a. In the first stage, the incipient cyclone presents a narrow and long cold front, and a wide and short warm front (Figure 2.4aI). After this, the cyclone deepens, with a narrowing of the warm section of the cyclone through the rotation of the cold front towards the warm front (Figure 2.4aII). As cold air is denser and, therefore, facilitates more intense horizontal pressure gradients, it moves faster than the warm air. As the cold air at the front of the cyclone approaches the cold air at the rear of the system (Figure 2.4aIII), the warm air is trapped in the center of the system, a phenomenon called warm seclusion. As the cold front continues to move, the warm air at the surface is overtaken by the cold air and is forced to ascend to upper levels. This process is called occlusion, being responsible for trapping the cold air in the core of the system (Figure 2.4aIV). With the continuation of occlusion, the baroclinicity along the warm front can become so diffuse that the cyclone appears not to have a well-defined warm front.

Bjerknes and Solberg (1922) acknowledged that the model presented in Bjerknes (1919) captured only a singular phase in the life cycle of cyclones, leading to the development of the Polar Front Theory. This theory defines what is known as the Norwegian cyclone model. Schultz et al. (1998) provides a synthesis of extratropical cyclone development according to this theory, including a depiction of the surface horizontal structure at various stages of cyclone evolution in Figure 2.4a. Initially, the nascent cyclone features a narrow, elongated cold front and a broader, shorter warm front (Figure 2.4aI). Subsequently, the cyclone deepens as the cold front rotates toward the warm front, narrowing the cyclone's warm sector (Figure 2.4aII). Given the greater density of cold air, which generates stronger horizontal pressure gradients and moves more swiftly than warm air, the cold front eventually encroaches on the system's rear cold air (Figure 2.4aIII), trapping warm air at the system's center—a process known as warm seclusion. As the cold front progresses, the surface-level warm air is displaced by cold air and forced upward, a phenomenon termed occlusion, which entraps cold air at the system's core (Figure 2.4aIV). The occlusion process may eventually diffuse the baroclinicity along the warm front to such an extent that the cyclone seems to lack a distinct warm front.

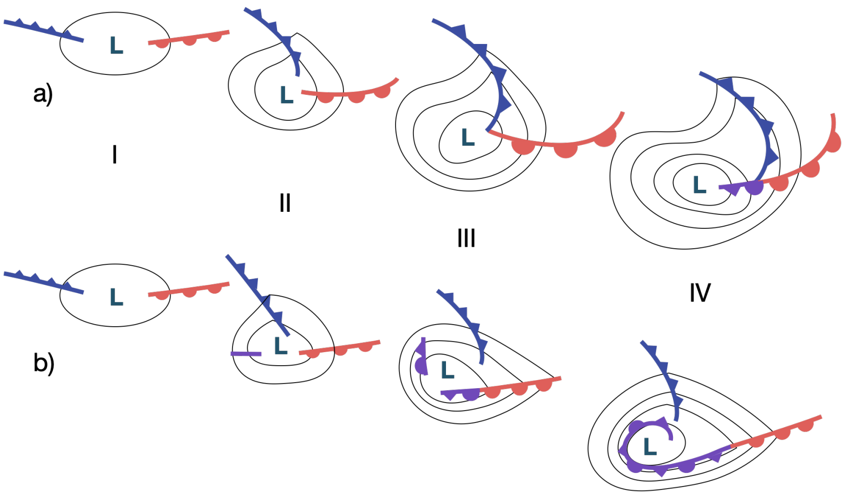

Figure 2.4: Cyclonic models by Bjerknes (1919) (a) and Shapiro and Keyser (1990) (b), illustrating the systems' horizontal structure across different developmental stages (I to IV). Adapted from Schultz et al. (1998).

From the advancements enabled by the satellite era, Shapiro and Keyser (1990) introduced a revised cyclonic model, acknowledging that not all observed cyclones conformed to the Norwegian model. Termed the Shapiro-Keyser model, it is also summarized by Schultz et al. (1998), with its visualization in (Figure 2.4b). Initially mirroring the development outlined by Bjerknes and Solberg (1922) (Figure 2.4bI), this model diverges as the cold front extends perpendicularly to the warm front instead of encircling the system (Figure 2.4bII). As the system strengthens, the polar side of the cold front weakens, allowing the warm front to encircle the system's western sector (Figure 2.4bIII). At peak intensity, cold air encases the warm air near the cyclone's center, creating a warm seclusion (Figure 2.4bIV).

Schultz et al. (1998) emphasizes that these models are complementary rather than mutually exclusive, suggesting that the Norwegian model is more applicable to systems forming under diffluent flow with significant amplitude, often at the terminal end of storm tracks and on western continental edges, characterized by a meridional elongation of the cyclone and its fronts. Conversely, the Shapiro-Keyser model is more suited to systems emerging under confluent, low amplitude base flow, typically exhibiting east-west elongation. However, these models alone do not fully account for the formal causes of extratropical cyclones, indicating a continuum where different systems may align more closely with one model or the other (Schultz et al., 1998).

Tropical cyclones, unlike their extratropical counterparts, lack frontal structures and exhibit organized, symmetric circulation near the surface, forming over warm tropical or subtropical waters with intense winds below the surface (Frank, 1977a; Gray, 1968). Their diameters vary, ranging from 100 to 1000 km at maturity, expanding up to 2000 km during intensification. However, the area of intense convection and stronger winds typically spans a radius of about 100 km (Holton, 1973).

Characterized by a central cyclonic circulation at lower tropospheric levels and anticyclonic circulation in the upper troposphere, tropical cyclones are associated with intense precipitation and horizontal pressure gradients, leading to spiraled winds near the surface that become increasingly circular towards the system's center, or eye (Frank, 1977a,b; Terry, 2007; Weatherford and Gray, 1988). These systems exhibit more intense pressure gradients—and consequently stronger winds—than extratropical cyclones (Spiridonov and Ćurić, 2021). Based on wind speed, they are classified into tropical depressions (maximum winds less than 60 km/h), tropical storms (winds between 60 and 110 km/h), and tropical cyclones (winds exceeding 110 km/h) (Spiridonov and Ćurić, 2021). Their nomenclature varies by region: "hurricanes" in the North Atlantic and North Pacific, "typhoons" in the Northwest Pacific, and "cyclones" in the Indian Ocean (Donald Ahrens and Henson, 2015).

The structure of tropical cyclones comprises three main components: the eye, the eye wall, and surrounding convection bands (Figure 2.5). The eye is the calm, warm central region, with a radius of 5 to 50 km, encircled by the eye wall—a cloud ring about 10 to 20 km wide where intense upward vertical movements occur, facilitating mass transport to higher levels (Shea and Gray, 1973; Jorgensen et al., 1985). Although these vertical movements are typically less vigorous than those in extratropical cyclones (Jorgensen et al., 1985), the inner core, consisting of the eye and eye wall, hosts the most intense winds and lowest atmospheric pressures (Weatherford and Gray, 1988). The primary convection band, a nearly stationary feature, spirals inward from the system's outer edges towards the eye wall, where it becomes roughly tangent (Willoughby et al., 1984).

Given the delineated formal causes (organizational structure) for both extratropical and tropical cyclones, it's evident that their structures diverge significantly. Simplified, extratropical cyclones, forming at the interface between distinct air masses, are associated with frontal systems, providing them an asymmetric feature. Conversely, tropical cyclones

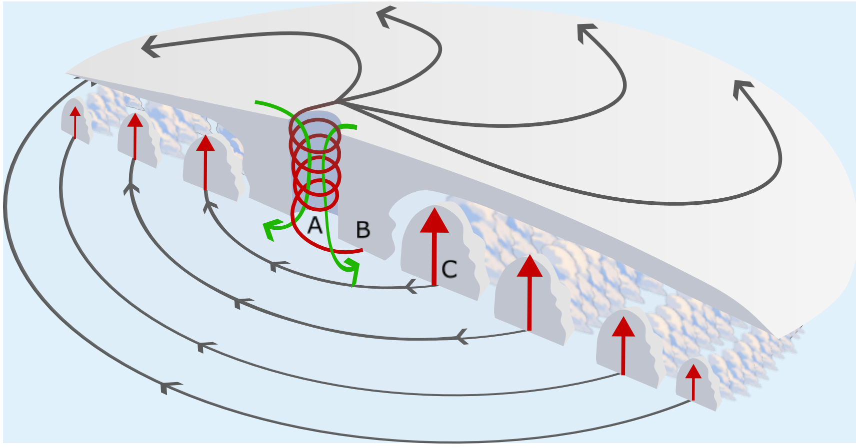

Figure 2.5: Cross-sectional view of a mature tropical cyclone in the Southern Hemisphere, illustrating the eye (A), eye walls (B), and convection bands (C), along with upward (red arrows) and downward (green arrows) vertical movements, horizontal wind movement (grey arrows), and sea-level pressure contours. Inspired from: Bluestein (1992).

exhibit symmetry, characterized by a circular eye and spiraled convection bands extending from the eye wall. Addressing this distinction, Hart (2003) introduces a metric assessing the relative thickness asymmetry between the 900 and 600 hPa levels, termed the B parameter:

$$B = h\left(\overline{Z_{600hPa} - Z_{900hPa}}|_R - \overline{Z_{600hPa} - Z_{900hPa}}|_L\right) \tag{2.5}$$

where Z represents the isobaric height, R and L denote the right and left sides relative to the system's motion, the overbar signifies an average over a 500 km semicircle, as defined in Equation 2.1, and h is a constant set to +1 or -1 for the northern and southern hemispheres, respectively. Mature tropical cyclones exhibit a B value near zero, indicating thermal symmetry (non-frontal), while extratropical cyclones show significant B values, signaling thermal asymmetry (frontal). Positive B values suggest the presence of warm air to the right of the cyclone in the southern hemisphere (and vice versa in the northern hemisphere), aligning with the thermal wind relationship from quasi-geostrophic theory (Sutcliffe, 1947; Trenberth, 1978).

Hart (2003) proposed a diagram correlating symmetry with V_T^L (Equation 2.4), depicted in Figure 2.6, offering a supplementary classification to that shown in Figure 2.2. Here, extratropical cyclones are categorized as cold and asymmetric (frontal), whereas tropical cyclones are warm and symmetric (non-frontal). Like the earlier diagram, this classification suggests a continuum, with systems displaying intermediate features labeled as subtropical.

Unlike solely thermal-based classifications, this model allows for differentiation of extratropical cyclones undergoing occlusion, as these systems begin to exhibit symmetry during this phase. Hence, the diagram involving the B parameter and V_T^L presents an objective methodology to classify cyclones' formal causes.

While the phase diagrams by Hart (2003) facilitate objective classification criteria for cyclonic systems, gaps remain. For instance, warm seclusions share formal and material causes with hybrid systems, leading to potential misclassification by forecasters and climate data analysis algorithms using these diagrams exclusively. Additionally, polar lows, characterized by both a warm core and symmetric structure, were initially likened to hurricanes (Rasmussen, 1989; Emanuel and Rotunno, 1989; Nordeng and Rasmussen, 1992; Rasmussen, 1985, 1979). However, recent studies, such as Stoll et al. (2021), suggest their spiral bands and thermal core may result from the warm seclusion process, as per the Shapiro-Keyser cyclone development model. These discussions underscore that material and formal causes alone do not suffice for a comprehensive cyclone classification, necessitating further analysis.

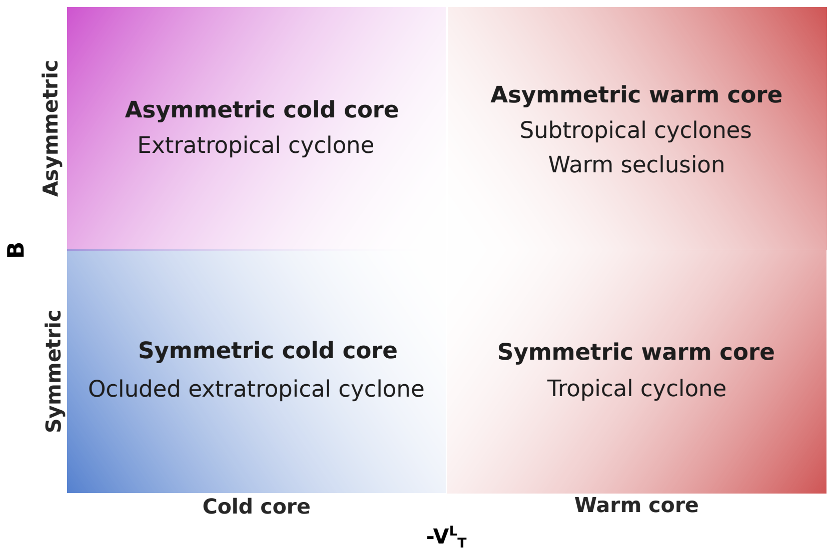

Figure 2.6: Phase diagram illustrating the relationship between cyclonic systems' core temperature and symmetry, offering a distinct classification procedure. Adapted from Hart (2003).

2.1.3 Efficient Causes

The efficient cause represents the agent or process that leads to the creation or transformation of something, answering the "how" or "why" behind an occurrence. It encompasses the actions or processes that result in the existence of an entity. For example, in the creation of a table, the carpenter serves as the efficient cause. In the context of cyclones, the efficient cause includes the physical and dynamic processes responsible for their formation and intensification. These processes essentially act as destabilization mechanisms, triggering atmospheric disturbances that evolve into a cyclonic configuration.

While the polar front theory offers a descriptive perspective, it falls short of providing a comprehensive theoretical model for the physical processes involved in system formation. Still, it related these processes with thermal contrasts in the atmosphere, or baroclinic zones (Bjerknes, 1919; Bjerknes and Solberg, 1922), describing cyclones as emergent phenomena arising at the boundary of two distinct air currents—polar and tropical—flowing in opposite directions (east-west and west-east, respectively), differentiated by thermal contrasts (cold and warm, respectively). A destabilization of the flow occurs when the velocity difference between these currents surpasses a critical threshold, generating a frontal wave that intertwines the currents and reduces their velocity contrast. Some of these frontal waves are unstable and can spontaneously amplify, representing the genesis mechanism of cyclones according to this theory.

The Polar Front Theory provides a detailed account of the structure and formation processes of extratropical cyclones, as shown in Figure 2.7, depicting a transverse model of a developing cyclone (Bjerknes and Solberg, 1922). This model features horizontal isotherms indicative of temperature variations parallel to the ground, with warm air central to the model, characteristic of the warm front, and cold air on the edges. Initially (Figure 2.7a), the isotherms of cold air extend horizontally until convergence forces the ascent of warm air to higher atmospheric levels. This conversion of potential to kinetic energy continues as the cold air from both sides of the cyclone advances to mid-atmospheric levels, further driving the ascent of warm air. The adiabatic cooling of ascending warm air leads to temperature equalization and depletion of the system's potential energy reserve, while the air mass movement is then sustained by inertia. After occlusion (Figure 2.7b and c), inertia maintains the ascent of cold air, which cools adiabatically, utilizing the system's kinetic energy to counteract gravity. Initially, there is still kinetic energy production at high levels and its consumption at low levels. However, as the elevated warm sector cools and temperatures equalize (Figure 2.7d), kinetic energy production halts. Eventually, friction outweighs kinetic energy production, leading to its dissipation.

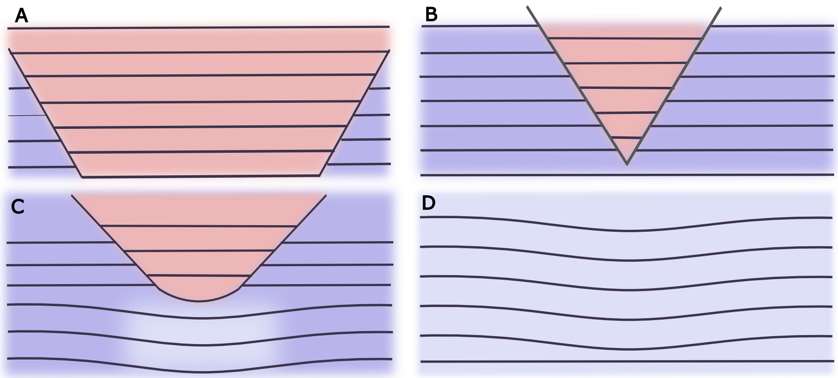

Figure 2.7: Cross-sectional depiction of an extratropical cyclone's development through its various stages, adapted from Bjerknes and Solberg (1922). Stage A shows horizontal isotherms where cold air converges, leading to the ascent of warm air. In Stage B, the system begins occlusion as cold air advances to mid-atmospheric levels, further promoting the ascent of warm air. Stage C continues the occlusion, with sustained ascent of cold air by inertia and kinetic energy consumption. Stage D represents the cessation of kinetic energy production as temperatures equalize and friction begins to dominate, leading to energy dissipation. Warm (red) and cold (blue) sectors are indicated alongside the isotherm lines.

Since the advent of the polar front theory, our comprehension of atmospheric dynamics has evolved significantly, incorporating new concepts into the understanding of extratropical cyclones. This evolution has led to a diverse array of approaches aimed at describing the dynamic and thermodynamic processes underlying the genesis and development of these systems. Consequently, there is no singular, unified theory regarding extratropical cyclogenesis. For instance, Bjerknes and Holmboe (1944) identified the formation regions of extratropical cyclones as zones of dynamic instability associated with the westward-flowing jet stream, employing the tendency equation to analyze atmospheric instability. Other studies have approached cyclogenesis through various lenses, including slantwise convection, the omega equation, potential vorticity, primitive equations, and diabatic processes (Hoskins, 1990, e.g.). Additionally, Schultz et al. (1998)'s work categorizes cyclones into those aligning with the Norwegian model versus the Shapiro-Keyser model, differentiating them based on environmental conditions related to the base state flow (diffluent for the former and confluent for the latter). This section will primarily focus on the development of these systems from the perspective of dynamic destabilization mechanisms in the atmosphere, linking these mechanisms to the energetics of transient atmospheric systems, further explored in Section 2.4.

Baroclinic instability (I_{BC}) is identified as the principal mechanism behind the development of typical extratropical cyclones (Charney, 1947; Bjerknes and Solberg, 1922). As Holton (1973) explains, I_{BC} involves the amplification of small disturbances in areas with strong velocity shears, such as jet streams, where the disturbances extract energy from the jet and grow in size and intensity. In the Earth's atmosphere, I_{BC} is primarily driven by the meridional temperature gradient, especially at lower levels, and is linked to vertical shear via the thermal wind (V_T) relationship, frequently occurring in the polar frontal zone. Baroclinic disturbances can also intensify existing temperature gradients, leading to the formation of frontal zones.

Charney (1947)'s seminal study on I_{BC} sheds light on the intricate mechanisms behind the formation and evolution of weather patterns, including cyclones and long waves in middle and high latitudes. Employing a simplified model that allows for analytical solutions, Charney not only corroborated previously theorized concepts about atmospheric behavior but also deepened the understanding of how wind shear and temperature variations vertically contribute to atmospheric instability. His analysis indicates that mid-latitude westward-flowing currents are inherently dynamically unstable. This insight elucidates how specific disturbances can exponentially grow within a large-scale atmospheric flow field, explicating the process through which such disturbances can amplify and culminate in the characteristic weather systems observed in middle and high latitudes.

Eady (1949) made significant advancements in the understanding of I_{BC} in the atmosphere, building on the work of Charney (1947). Eady's research, which employed a solvable simplified model, delved into the atmospheric instability arising from disturbances that exponentially grow within a large-scale atmospheric motion context. His analysis elucidated how specific conditions of stability, wind shear, and vertical temperature variations contribute to I_{BC}, proposing a mechanism for the formation and evolution of weather patterns such as cyclones and long waves in middle and high latitudes. Eady highlighted that certain disturbances grow exponentially faster than others, akin to a process of natural selection in the atmosphere, leading to the emergence of predominant weather patterns observed in middle latitudes, including cyclonic systems.

Following the seminal works of Charney (1947) and Eady (1949), Palmén and Newton (1969) synthesized the main findings from the subsequent extensive literature on I_{BC}. Firstly, it is noted that the amplification of atmospheric disturbances is wavelength-dependent, with disturbances below a critical length never amplifying. The optimal growth occurs in intermediate wavelengths (between 2500 and 5000 km), with an inverse relationship between this optimum and latitude—the closer to the Equator, the larger the critical size below which all waves are unstable. Additionally, there exists a proportional relationship between the intensification rate and vertical wind shear for wavelengths of maximum instability, and for longer waves, an increase in wavelength necessitates stronger shear to maintain equivalent growth rates.

In his analysis, Petterssen and Smebye (1971) categorizes extratropical cyclones into types based on the dynamic processes driving their development. Type A cyclones follow the Polar Front Theory model, with the initial disturbance arising at low levels within a maximal baroclinic zone (frontal), beneath a nearly zonal upper-level jet (Figure 2.8iA). As these cyclones develop, a cold trough forms at high levels (Figure 2.8iB), remaining inclined to the cyclone's axis until occlusion occurs and surface baroclinicity diminishes (Figure 2.8iC). Conversely, type B cyclones initiate from high-level forcing, as an upper-level trough moves over an area not necessarily featuring a frontal zone (Figure 2.8iiA). As these systems mature, the gap between the high-level trough and the surface system narrows, with an increase in surface baroclinicity relative to the initial stage (Figure 2.8iiB), culminating in the alignment of the high-level cyclonic vortex with the surface low, leading to system occlusion (Figure 2.8iiC).

Just as Hart (2003)'s classification presents a continuum, so too does Petterssen and Smebye (1971)'s delineation of cyclone types, with A and B not being distinct categories due to the existence of systems displaying hybrid characteristics. Petterssen and Smebye (1971) observed that purely type A cyclones are more common, whereas purely type B cyclones are rare, attributing this to the fact that some type of baroclinicity is often present in the mid-latitudes. However, Petterssen noted a tendency for type A cyclones to develop over oceans and type B cyclones over continents, though subsequent research, such as by McLennan (1988) and Deveson et al. (2002), has identified type B systems forming over oceanic regions as well. Furthermore, Deveson et al. (2002) introduced a new classification, type C cyclones, found in high latitudes with similarities to polar lows, characterized by an even stronger high-level forcing related to the movement of a broad trough over oceanic regions. This study also highlighted the potential for cyclones to transition between types throughout their lifecycle.

The central role of baroclinic instability (I_{BC}) in the development of extratropical cy-

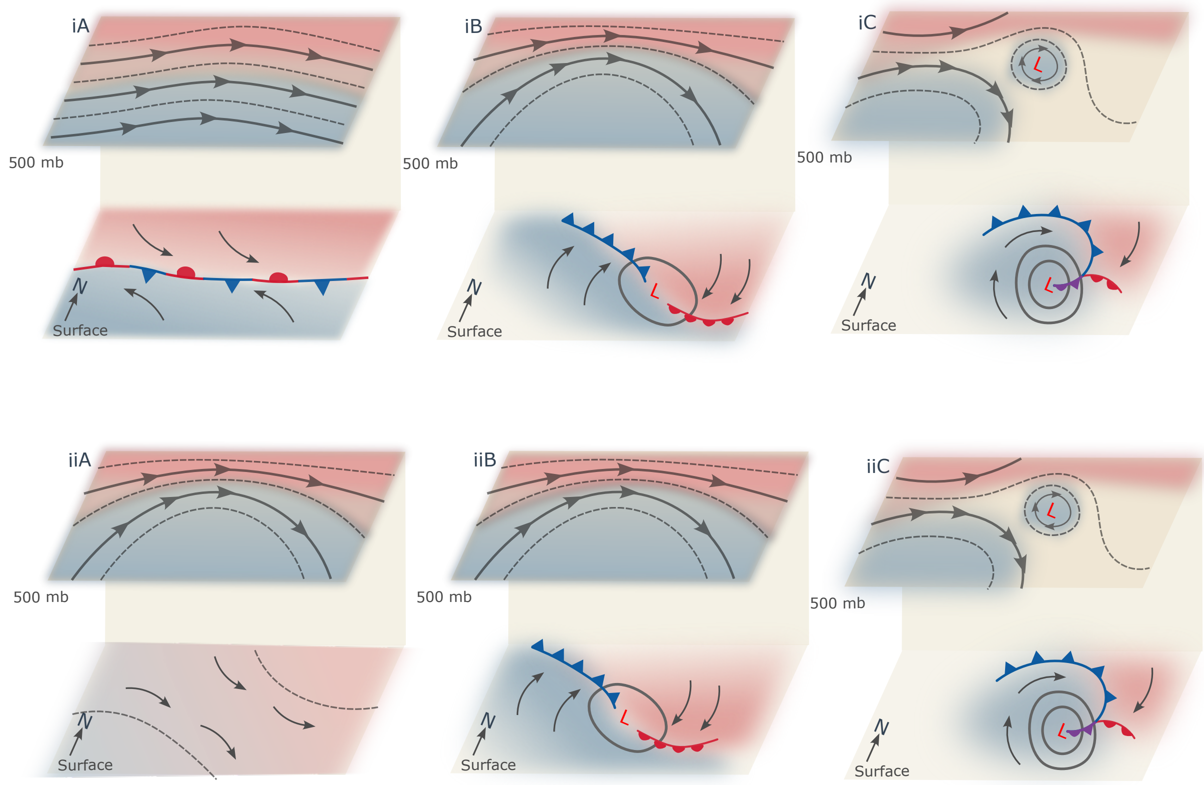

Figure 2.8: Illustration of the development model for cyclones types A (i) and B (ii), depicting the stages of formation (A), intensification (B), and maturity (C), as proposed by Petterssen and Smebye (1971). Inspired by Donald Ahrens and Henson (2015).

clones is well-established, yet the significance of heat flows and diabatic heating cannot be overstated. Diabatic heating involves heat exchanges between a system and its surroundings through processes such as condensation, evaporation, or radiation. Convective activities leading to upward atmospheric movements cause diabatic expansion and thus cooling in air parcels, leading to saturation and the release of latent heat. Such mechanisms provide an additional energy source for the development of extratropical cyclones, as documented in the literature (Chang et al., 2002, e.g.). Numerical models incorporating I_{BC} alongside heat flows have shown that instabilities generated under these conditions yield more intense cyclones with faster development rates (Gall, 1976; Whitaker and Davis, 1994; Gutowski et al., 1992), a phenomenon referred to as moist baroclinic instability.

A pivotal study by Hoskins and Valdes (1990) underscores the importance of diabatic fluxes in the development of extratropical cyclones, demonstrating that cyclonic development is preferentially located in regions of maximal baroclinicity over the oceans. However, the heat transport facilitated by these systems tends to mitigate the baroclinicity. The study suggests that diabatic heating, through the latent heat release from individual systems, contributes to sustaining regional baroclinicity. It also highlights the role of sensible heat exchanges between the cold air associated with these systems and the warm ocean currents along the eastern coastlines of continents.

Tropical cyclone formation, a topic of ongoing discussion among meteorologists, typically occurs over tropical or subtropical oceans, a region where the scarcity of in situ observations challenges the validation of theoretical models for formation and intensification. During World War II, data collected from the military base in Guam facilitated Riehl (1948) in proposing that the instability necessary for typhoon formation originates within the trade winds, contradicting the then-prevailing belief of inter-hemispheric air mass interactions being the primary cause. Subsequently, Yanai (1961)'s study on Typhoon Doris furthered the understanding of typhoon genesis, highlighting the significant role of latent heat released by convection. Yanai suggested a model for typhoon development, beginning with a disturbance in the trade winds and culminating in the formation of a typhoon characterized by a stabilized warm core.

Charney and Eliassen (1964) detailed the process of tropical cyclone intensification known as conditional instability of the second kind (CISK), which was the most accepted theory at the time (Figure 2.9i). According to CISK, the condensation of water vapor within convective areas releases latent heat, which can amplify pre-existing atmospheric vortices given an adequate moisture supply. This release of heat not only promotes further convection but also lowers sea-level pressure, thereby strengthening surface winds, enhancing moisture influx, and establishing a positive feedback loop. Charney underscored the ocean's surface role in providing the moisture necessary for sustaining convection, as well as the importance of surface friction in dissipating kinetic energy and fostering wind convergence within the moist surface boundary layer, thereby fueling the system with thermal energy from latent heat. This mechanism emphasizes the pivotal role of latent heat release at the cyclone's center as a disturbance amplification factor, leading to the intensification of the tropical depression.

However, it is important to note that the work of Charney and Eliassen (1964) consists of formulating a mathematical model and, therefore, does not offer a direct and didactic explanation of the processes involved. Thus, the interpretation of the proposed mecha-

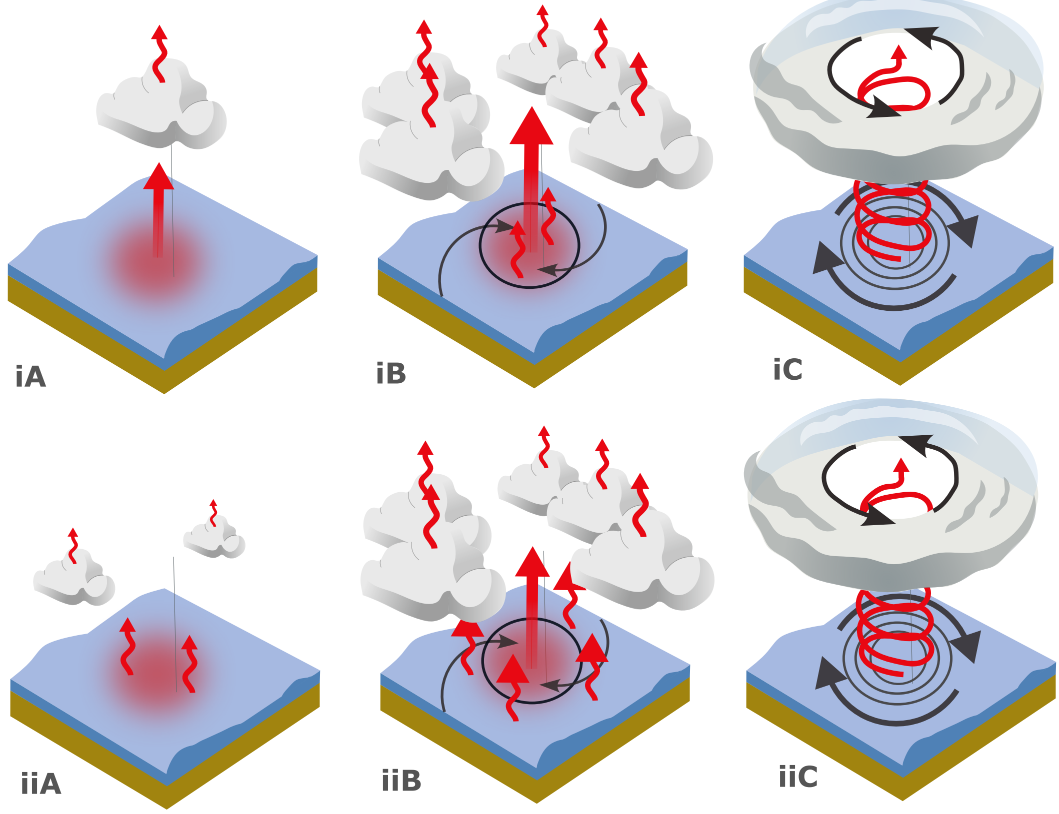

Figure 2.9: Comparative illustration of the CISK (i) and WISHE (ii) theories. A depicts the initial disturbance over warm ocean temperatures. Under CISK, the disturbance is initially fueled by latent heat from convection, whereas WISHE attributes the initial energy source to latent heat transfer from the ocean to the atmosphere. In the early development stage (B), both theories observe an increase in convection. CISK suggests this leads to reduced central pressure, drawing in more moisture and enhancing convection, which releases additional heat. WISHE proposes that surface wind interaction with the sea surface at low central pressure enhances heat release from surface water evaporation, further driving convection and subsequent latent heat release. By the tropical storm phase (C), the theories align on the feedback mechanisms fueling system intensification.

nisms is largely left as an exercise for the reader, which has resulted, over the years, in multiple interpretations, not all of them correct (Ooyama, 1982). Therefore, the explanation provided above seeks only to simplify the main processes proposed by Charney and Eliassen (1964).

While Charney and Eliassen (1964)'s work introduces a mathematical model for understanding tropical cyclone intensification through the CISK process, it doesn't offer a straightforward, didactic explanation of the involved mechanisms. This has left room for various interpretations over the years, not all of which have been accurate, as noted by Ooyama (1982). The explanation provided here aims to to simplify the main processes proposed by Charney's for clarity.

Challenging the CISK theory, Emanuel (1986), later refined by Yano and Emanuel (1991), introduced the Wind-Induced Surface Heat Exchange (WISHE) theory, emphasizing ocean-atmosphere interaction as the primary intensification mechanism for tropical cyclones (Figure 2.9ii). WISHE posits that the development of these systems depends on the thermal contrast between the atmosphere and the sea surface, mediated by latent heat transfer from the ocean to the atmosphere. This transfer is significantly amplified by surface wind speeds, with intense winds elevating evaporation rates and thus, moisture transfer. An initial atmospheric disturbance that promotes wind convergence toward its center can enhance this moisture transfer and convection intensity, fostering a positive feedback cycle. WISHE theory emphasizes the necessity of ocean temperatures exceeding 26°C for sufficient boundary layer convergence, vital for maintaining the system. Similar to CISK, interpretations of WISHE vary, with not all encapsulating the theory's full scope or accuracy (Montgomery and Smith, 2014); thus, the provided explanation concentrates on fundamental aspects for comparative purposes with CISK.

Despite advancements in identifying the prerequisites for tropical cyclone development—such as requisite sea surface temperatures, minimal vertical wind shear, and specific atmospheric conditions—consensus on the precise dynamic processes driving both formation and intensification remains elusive. This ongoing debate in meteorology is exemplified by the contrasting theories of CISK and WISHE, each proposing different intensification mechanisms for tropical cyclones (Craig and Gray, 1996; Gray, 1998; Montgomery et al., 2015; Ooyama, 1982; Montgomery and Smith, 2014, e.g.,). Nonetheless, a common point between them is the acknowledgment that diabatic processes, fueled by ocean-atmosphere interactions and given an initial disturbance, are critical for providing energy and further intensifying the system. This section's goal is to delineate the development mechanisms of tropical versus extratropical cyclones, for which the simplified descriptions provided herein offer an adequate overview.

The role of diabatic heating in the intensification of tropical cyclones is underscored by the need for an initial atmospheric disturbance. Frank (1970) conducted an analysis of systems in the North Atlantic that give rise to disturbances capable of developing into tropical cyclones. He identified several sources of these disturbances, including those originating from the Intertropical Convergence Zone (ITCZ) and convection zones within the Caribbean Sea. However, the majority are associated with tropical waves primarily emanating from the African continent. Frank also highlighted the process whereby baroclinic systems transition into warm-core structures through the convection-driven release of latent heat, effectively diminishing the system's original baroclinicity. This phenomenon is now recognized as the tropical transition of extratropical cyclones, a process further explored and detailed in works such as those by Hart (2003).

The genesis of tropical cyclones in the North Atlantic is intricately linked to the formation and development of African easterly waves, with the thermal contrast between the Sahara Desert and cooler southern regions playing a pivotal role in creating the African Easterly Jet (AEJ)—a key factor in generating these waves (Holton, 1973). The foundation for understanding such phenomena was laid by Kuo (1949), who pinpointed barotropic instability in zonal atmospheric flows as a vital mechanism. This instability, marked by a change in the sign of absolute vorticity, involves horizontal wind shear and allows vortexes to extract kinetic energy from the zonal wind flow (Holton, 1973).

Burpee (1972) initially connected African easterly wave development with the instability of the AEJ, due to both horizontal and vertical shears, pointing to the complex interaction between barotropic and baroclinic instabilities in the region. Following this, Rennick (1976) applied a linear pseudo-spectral model based on primitive equations, deducing that barotropic instability acts as a primary catalyst for wave development, while downplaying the roles of vertical shear and latent heat release in the early stages. This assertion was supported by Reed et al. (1977) through observational data, demonstrating that medium and low-level easterly waves meet the criteria for barotropic instability.

An energetic analysis by Norquist et al. (1977) differentiated the destabilization processes over land and ocean, with baroclinic conversion dominating over the continent and barotropic instability gaining importance over oceanic regions—where tropical cyclones predominantly form. More recently, Wu et al. (2012) employed reanalysis data to establish a geographical link between the AEJ's barotropic instability and the origination points of North Atlantic tropical cyclones, affirming the significance of the AEJ's barotropic instability in relation to tropical cyclogenesis.

The exploration of barotropic instability's role in tropical cyclone genesis extends beyond the North Atlantic, encompassing various global regions where similar dynamics foster local tropical cyclogenesis. While initial studies illuminated the significance of barotropic instability in the genesis of African easterly waves and their impact on North Atlantic tropical cyclone formation, subsequent research has broadened our understanding to include other tropical areas. For instance, Zehr (1992) discovered that most tropical cyclogenesis events in the North Pacific are associated with a monsoon trough that encourages local convection.

In addition to easterly waves, different types of tropical disturbances can also disrupt the base state and instigate tropical cyclogenesis. Ferreira and Schubert (1997) used a shallow water model to show how barotropic instability related to the ITCZ's collapse can initiate a series of tropical disturbances, with some progressing to become tropical cyclones. Further, Bembenek et al. (2021) employed a global aquaplanet circulation model to illustrate the significant roles played by the ITCZ's latitudinal position and moisture effects in modulating barotropic instability and, consequently, tropical cyclone genesis, indicating the global influence of barotropic instability on tropical cyclogenesis through theoretical studies.

Observational evidence supports these theoretical insights. Maloney and Hartmann (2001) observed that the Madden-Julian Oscillation (MJO) phases conducive to westerly winds along the Pacific enhance barotropic conversions at low levels, thereby aiding tropical cyclone formation in both the Western and Eastern Pacific. Molinari et al. (1997) noted that temporal variations in the MJO can create conditions favorable for easterly wave growth, thereby affecting tropical cyclogenesis in the Eastern Pacific. Molinari et al. (2000) identified a link between the barotropic instability of the base state, associated with easterly wave occurrence, topographical effects, and the monsoon trough in fostering tropical cyclogenesis in the Eastern Pacific. Lastly, Cao et al. (2012) found that enhanced ITCZ convection during active phases of the Intraseasonal Oscillation generates a mean flow state conducive to barotropic instability, promoting tropical cyclogenesis in the Northwest Pacific.

While subtropical cyclones were identified in earlier works (Simpson, 1952), it wasn't until the study by Hart (2003) that they began receiving significant attention. The body of literature on these systems is still developing, with the processes behind subtropical cyclogenesis and development remaining an active area of research. Yanase et al. (2014) advanced the understanding of cyclone genesis by developing an Environmental Parameter Space, analyzing how cyclone genesis latitude correlates with factors like baroclinicity, relative humidity, vertical velocity, and potential intensity. This last metric predicts a tropical cyclone's maximum possible strength based on environmental conditions such as sea surface temperature and atmospheric temperature profiles. The study found a clear correlation: extratropical cyclones are closely linked to baroclinicity, while tropical cyclones are associated with potential intensity. Conversely, an inverse relationship was noted—extratropical cyclones inversely relate to potential intensity and tropical cyclones to baroclinicity. Subtropical cyclones emerged in a transitional space, influenced by both baroclinicity and potential intensity, which supports the notion of these systems as hybrids between tropical and extratropical cyclones (Hart, 2003, e.g). Additionally, da Rocha et al. (2019) suggested that subtropical cyclogenesis could be linked to various synoptic patterns, such as a shallow trough at mid-upper levels, a mid-upper level cutoff low, or a Rex blocking pattern. However, a comprehensive discussion delineating the principal environmental dynamics associated with subtropical cyclone development remains elusive, indicating a need for further investigation in this area.

The discussion provided thus far can be synthesized by comparing the efficient causes related to the development of both extratropical and tropical cyclones. Extratropical systems primarily develop through baroclinic instability, which may be initiated by disruptions in the surface meridional temperature gradient or by the influence of an upper-level trough, linking to baroclinic regions via the thermal wind relationship (Holton, 1973; Spiridonov and Ćurić, 2021). In contrast, tropical cyclone genesis is largely influenced by barotropic instability within the base state atmosphere, with subsequent disturbances intensifying through processes related to latent heat release, as explained by either CISK or WISHE theories.

This comparison illustrates that extratropical cyclone formation is closely tied to thermal variance driving baroclinic instability, whereas tropical cyclone genesis hinges on barotropic instability, succeeded by a reinforcing latent heat release feedback mechanism. Despite the absence of a unified diagram akin to Hart (2003)'s material and formal causes of cyclones, Silva Dias et al. (2004) proposed a conceptual model potentially bridging this gap (Figure 2.10). This model situates extratropical cyclones within the domain of baroclinic instability; tropical cyclones under barotropic instability; and subtropical cyclones where both instabilities might coexist or compete. The model also distinguishes systems by their reliance on diabatic processes, particularly latent heat release.

The viewpoint of Silva Dias et al. (2004) gains partial validation through Yanase et al. (2014)'s analysis, which linked different cyclone types to specific environmental parameters. Furthermore, Yanase et al. (2014) emphasized the critical role of relative humidity across all cyclone categories, supporting Silva Dias et al. (2004)'s emphasis on the essential role of latent heat release in cyclone dynamics. The current study will introduce a conceptual model, detailed in Chapter 5, aiming to synthesize the primary mechanisms driving cyclonic development and explore their broader implications.

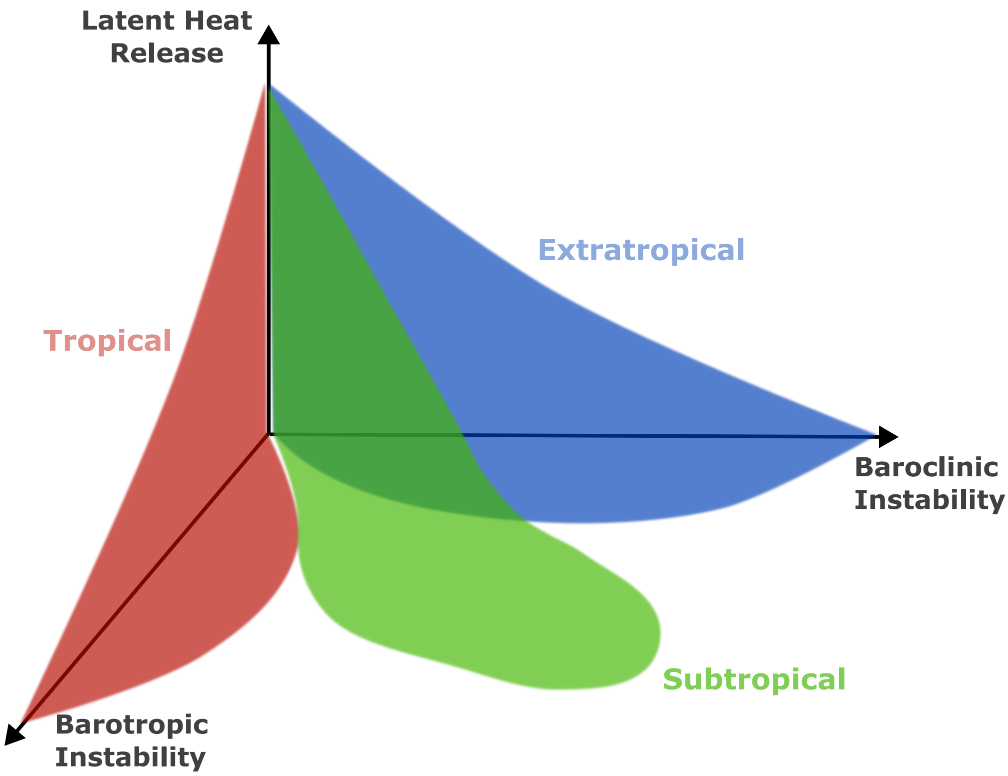

Figure 2.10: Proposed conceptual model correlating atmospheric destabilization mechanisms with cyclone types. Each axis within the three-dimensional schema represents a different process of atmospheric destabilization, allowing the categorization of cyclone types across the spectrum. Adapted from Silva Dias et al. (2004).

2.1.4 Final Causes

Final causes delve into the purpose or ultimate reason for the existence of something, offering insights into the "why" behind its occurrence. For instance, the final cause of a table is to serve as a platform for activities such as writing, eating, or working. When considering cyclones, their final cause could be viewed as the facilitation of heat and moisture redistribution within the atmosphere, thus playing a crucial role in maintaining global climatic equilibrium and acting as a mechanism for dissipating excess heat.

The Earth's climate system is fundamentally driven by solar radiation, while simultaneously losing heat through infrared radiation emitted into space. The unequal distribution of solar radiation, exacerbated by the tilt of the Earth's axis, results in energy surpluses in equatorial regions and deficits in polar areas. This differential heating prompts the formation of warm air masses near the equator and cold air masses in polar regions, instigating atmospheric circulation as an effort to achieve thermal equilibrium, a state that remains elusive due to ongoing differential heating between tropical and polar zones.

Historical and recent advancements in atmospheric science have underscored the significance of general atmospheric circulation in climate dynamics (Lorenz, 1967; Hadley, 1735; Stull, 2015; Schneider, 2006). The Hadley Cell emerges as a critical response to the disparity in solar radiation received at the equator compared to the poles (Figure 2.11). Warmed air rises near the equator, creating low-pressure zones at the surface and high pressure aloft. This ascending air, replaced by cooler air from higher latitudes, moves poleward at elevated altitudes due to mass conservation. The conservation of angular momentum is crucial as this air, moving away from the equator (where surface rotational speed is maximum), must increase its eastward velocity as it approaches the poles. This dynamic leads to the formation of subtropical jet streams around 30° latitude. The Polar Cell, integral to high-latitude atmospheric circulation, is driven by the thermal contrast between the poles and regions at 60° latitude. This temperature difference induces opposing north-south pressure gradients, generating equatorward winds that, due to the Coriolis force, become polar easterlies. At higher levels, winds flow poleward but are deflected eastward, forming an upper-level westerly flow around the polar low, thus completing the Polar Cell circulation.

Together, the Hadley and Polar Cells underscore a comprehensive circulation pattern that transports warm air and angular momentum from the equator towards the poles and vice versa, facilitating Earth's energy balance. Although initially conceptualized as symmetrical circulations extending from the equator to the poles, subsequent research has emphasized the pivotal role of large-scale eddies in heat and angular momentum transfer (Schneider, 2006). These eddies, critical to atmospheric dynamics, emerge due to baroclinic zones in mid-latitudes and are intrinsic to the structure and function of the Ferrel Cell in

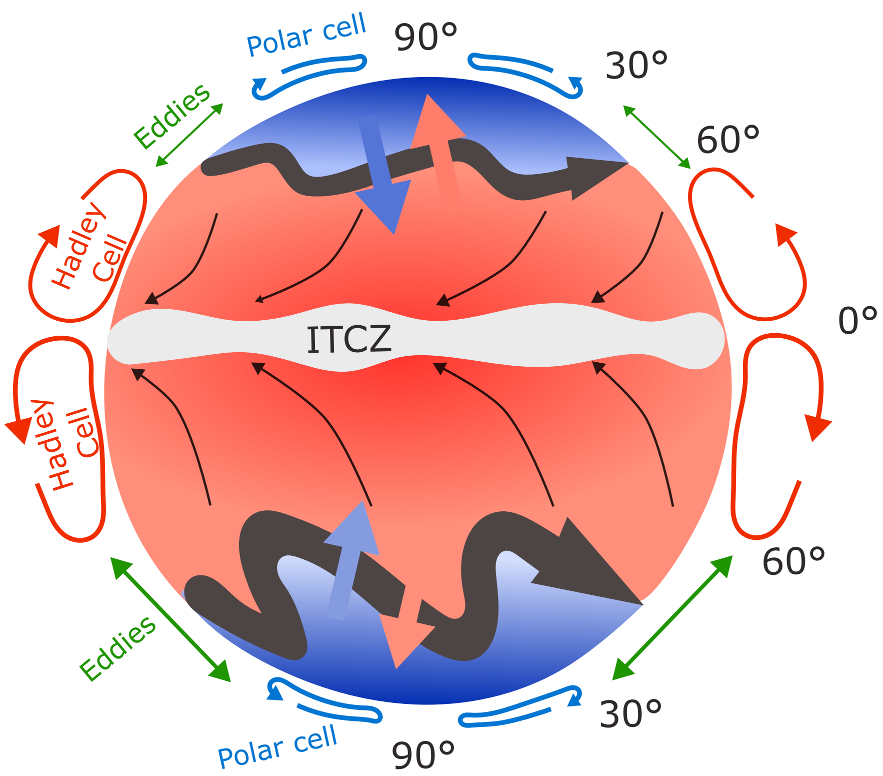

Figure 2.11: Representation of the global circulation pattern, showing the Hadley Cell circulation prominent at low latitudes, the transport of momentum and heat by eddies at mid-latitudes, and the polar cell circulation at high latitudes. Inspired by Stull (2015).

mid-latitudes(Held, 1999; Schneider, 2006). Arising from mid-latitude baroclinic zones, they are indispensable to the Ferrel Cell's operation, influencing wind patterns across latitudes and enhancing heat transfer between the tropics and poles (Stull, 2015; Held, 1999).

Due to their relatively small scale compared to extratropical cyclones, tropical cyclones are not directly associated with the three-cell model of global circulation. They arise in regions of low baroclinicity, where thermal contrasts are minimal, relying instead on the atmosphere's ability to generate energy from internal heat sources. These sources are largely the warm temperatures of tropical oceans and the air above them (Palmén and Newton, 1969). Often conceptualized as a Carnot heat engine (Figure 2.12), tropical cyclones draw heat from the ocean surface—primarily through the latent heat of vaporization—and release it into space via longwave radiation (Emanuel, 1987; Ozawa and Shimokawa, 2015; Wang et al., 2022, e.g.,). The cyclone's intensity depends on the efficiency of this heat engine, which is determined by the temperature difference between the heat source (ocean) and sink (upper atmosphere). Friction, especially near the ocean surface within the boundary layer, plays a crucial role by causing energy loss that can lessen wind speeds and alter angular momentum, impacting the cyclone's energy conversion efficiency.

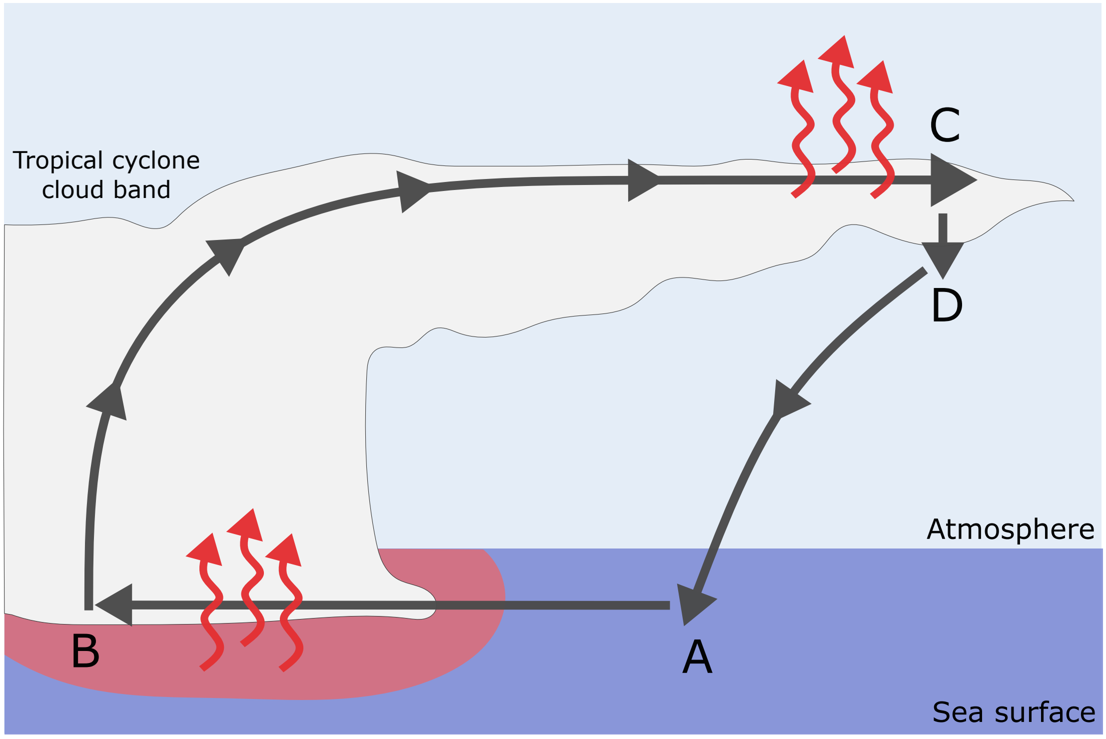

Figure 2.12: Diagrammatic Representation of a Tropical Cyclone as a Carnot Heat Engine. The process begins with isothermal inflow (A-B) at the surface, drawing energy from warm ocean waters into the cyclone's core. This stage is succeeded by the upward movement of air (convection) and outward flow just below the tropopause, characterized by radiative cooling and energy loss (B-C). Subsequently, cooled air descends away from the cyclone's center (C-D) and cycles back towards the cyclone, completing the circuit (D-A). Adaptation based on the COMET Program.

We can see then that tropical cyclones serve to dissipate excess heat in the tropics, utilizing oceanic heat to fuel the system while dissipating energy through radiation at the upper levels or friction at the surface. Given this model's applicability, Emanuel (1987) predicted that rising atmospheric CO_2 levels would lead to more intense tropical cyclones in the future. Recent climate models suggest an increase in tropical cyclone intensity, though there's no global consensus on frequency changes (Knutson et al., 2010; Walsh, 2004; Walsh et al., 2016, 2019). As discussed in Section 2.1.3, understanding tropical cyclone development remains a significant scientific endeavor, complicating precise predictions of their response to climate change and their regulatory effect on climate.

In exploring subtropical cyclones, much remains to be discovered. The global distribution of cyclonic activity exhibits a bimodal pattern, with tropical cyclones forming in tropical regions and extratropical cyclones in mid-latitudes, leaving subtropical areas relatively calm in terms of cyclonic development (Yanase et al., 2014). It's speculative—emphasis on "speculate"—to suggest that subtropical systems share the final causes of their tropical and extratropical counterparts, acting to erase thermal gradients by redistributing heat globally or dissipating excess heat. However, subtropical cyclones might perform these functions under hybrid environmental conditions, possibly moderating gradients in regions with an abundance of heat. Ongoing research into subtropical cyclones promises to provide further clarity on their impact on global circulation patterns and their role within the broader climatic system.

2.1.5 Summary

This section has explored the Aristotelian causes as they pertain to cyclones, comparing the various types—extratropical, tropical, and subtropical—while also acknowledging the existence of other cyclonic phenomena like warm seclusions and polar lows. For succinctness, the discussion primarily centered on the main types, suggesting that cyclonic systems form a continuum: extratropical systems at one end, tropical cyclones at the other, and subtropical systems exhibiting hybrid characteristics.

Initially, we discussed that cyclones' material causes are linked to the air masses constituting them. Extratropical cyclones are associated with cold cores throughout the troposphere, whereas tropical cyclones are characterized by warm cores. Subtropical cyclones, however, display warm cores at the surface and cold cores at higher tropospheric levels.

Regarding formal causes, the cyclones differ in structure. Extratropical cyclones, identified by their frontal features, show asymmetry. Tropical cyclones, described as symmetric, feature convection bands spiraling the central eye. Subtropical cyclones, meanwhile, may present a range of spatial configurations, neither fully asymmetric nor symmetric.

Efficient causes, the dynamic mechanisms behind cyclone development, vary. Extratropical cyclones are primarily driven by baroclinic instability, a comprehensive mechanism underlying their formation. Tropical cyclone genesis and intensification lack a unified theoretical model, with current theories suggesting that barotropic instability in tropical waves—coupled with diabatic processes like latent heat release—might describe their development. Subtropical systems, given the incipient state of research, are speculatively linked by the author to both baroclinic and barotropic instabilities, with diabatic heat playing a role.

The final causes reflect cyclones' contributions to global circulation. Extratropical cyclones are recognized for redistributing heat, mitigating temperature gradients in mid-latitudes. Tropical cyclones, functioning as thermal engines, dissipate excess heat in tropical regions. The role of subtropical cyclones in the climate system remains speculative; they are hypothesized to simultaneously embody the functions of the other two types.

One important feature noted is that most classifications adopted for cyclone classification are based on Hart (2003) diagrams that objectively distinguishes these systems based on their material and formal causes. Although much knowledge exists regarding the efficient and final causes of tropical and especially extratropical systems, such objective criterion for these causes is still lacking. The current research proposes such objective classification procedure in the hopes of aiding the investigation of such causes related to cyclonic systems.

A notable point is the reliance on Hart (2003)'s diagrams for cyclone classification, objectively differentiating systems by their material and formal causes. While extensive knowledge exists on the efficient and final causes of tropical and particularly extratropical systems, a clear criterion for these causes is absent. This work proposes an objective classification procedure to aid in investigating cyclonic systems' related causes.

2.2 Cyclones in South America

This section transitions to examining cyclonic phenomena within South America, with a particular emphasis on systems originating in or adjacent to this region. While previous sections have provided a comprehensive overview of various cyclone categories, their structures, formation mechanisms, and roles in atmospheric circulation, here we delve into cyclonic systems that have genesis in South America or its neighboring oceanic regions. Although systems originating along the western coast of South America are noted (Crespo et al., 2023, e.g.,), our primary focus is on cyclones forming in the southern and eastern sectors of South America and the Southeastern Atlantic region. These systems significantly influence the regional climate, particularly in South and Southeastern Brazil (de Souza et al., 2022; Reboita et al., 2010, e.g.), and can cause extreme weather events (Cardoso et al., 2022; de Souza and da Silva, 2021; Gramcianinov et al., 2020, e.g.). From this point on, we refer to this region encompassing the Southeastern Atlantic and the adjacent South American region as SESA.

2.2.1 Climatological aspects

The first cyclone climatology for SESA region was performed by Gan and Rao (1991), utilizing sea level pressure data from surface charts spanning a decade. Despite methodological constraints, the authors identified two primary cyclogenesis regions: one over Uruguay and another in Southeast Argentina, with the latter being more active in austral summer and the former in winter. They hypothesized that the cyclogenesis in these regions was driven by baroclinic instability of the westerlies and lee cyclogenesis—cyclogenesis influenced by the interaction between baroclinic disturbances and topography (Gan and Rao, 1994; Tibaldi et al., 1980).

Later studies, employing automated techniques to detect cyclones' minimum central pressure, validated the cyclogenesis regions identified by Gan and Rao (1991) (Simmonds and Murray, 1999; Simmonds and Keay, 2000; Mendes et al., 2010). Meanwhile, analyses based on relative vorticity fields, as opposed to minimum central pressure, found a third significant cyclogenesis area near Southeast Brazil (Hoskins and Hodges, 2005; Sinclair, 1995; Reboita et al., 2010; Gramcianinov et al., 2019). The shift towards relative vorticity for cyclone tracking, as discussed by Hoskins and Hodges (2002); Sinclair (1994), offers several technical advantages. In mid-latitudes, the background pressure gradient's intensity can foreshadow closed isobars in developing cyclones, making it challenging to detect cyclones until they intensify or reach higher latitudes. Thus, employing relative vorticity enables the identification of weaker and faster-moving systems, as well as cyclones in their nascent stages, when closed isobars might not yet be evident.

In the SESA region, previous research has successfully identified three key areas of cyclogenesis, and this current study will adopt the nomenclature established by Gramcianinov et al. (2019) for consistency and clarity. The ARG region, situated in Southeast Argentina, emerges as the most active, with a relatively steady cyclogenesis rate throughout the year, though it peaks during the austral summer (Crespo et al., 2021; Gramcianinov et al., 2019; Reboita et al., 2010). The LA-PLATA region, over the La Plata River basin, ranks second in genesis density, displaying heightened activity in the austral winter (Crespo et al., 2021;

Gramcianinov et al., 2019; Reboita et al., 2010). It's noteworthy that Reboita et al. (2010) identified the LA-PLATA region along the Uruguayan coast rather than over the continent, influenced by the application of a continental mask in cyclone tracking, which biases detection towards maritime regions. The final region, SE-BR, located near the Southeastern Brazilian coast, records the fewest genesis events, with a significant increase in activity during the austral summer compared to winter (Reboita et al., 2010; Gramcianinov et al., 2019; Crespo et al., 2021). Figure 2.13 summarises these findings.

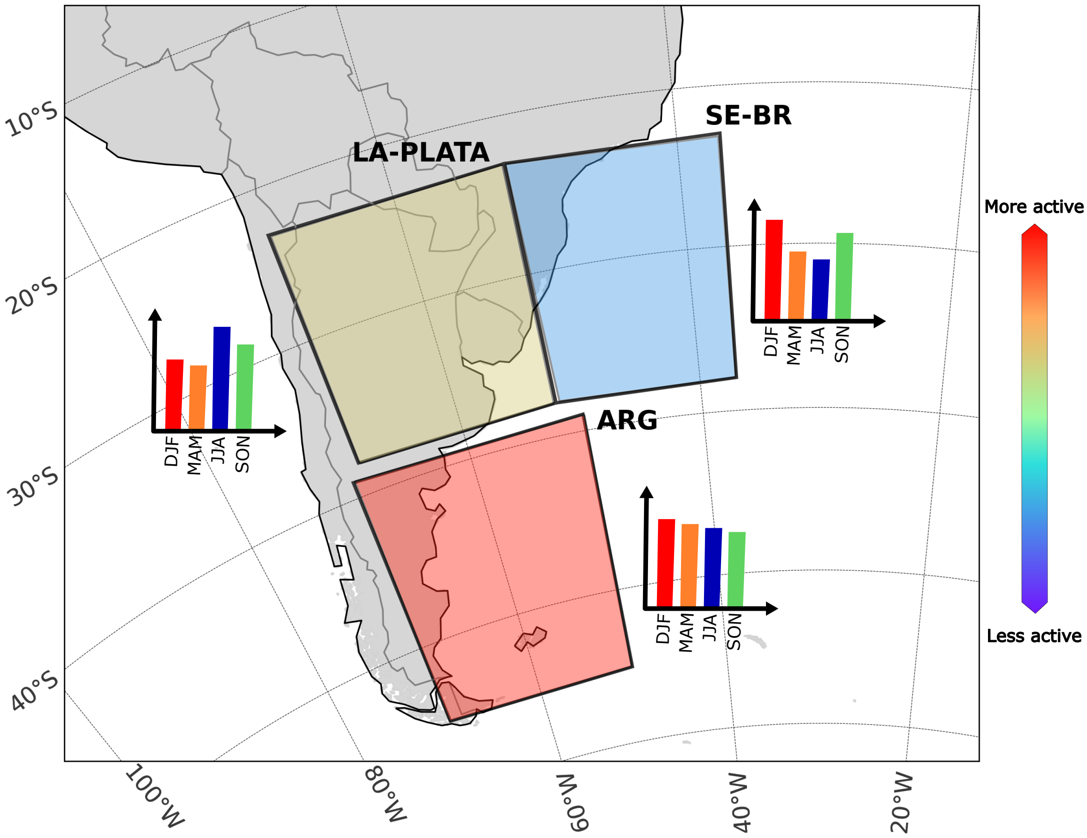

Figure 2.13: Illustrative mapping of cyclogenesis activity within the South American/Southeastern Atlantic (SESA) region, categorized into three primary genesis areas: ARG (Southeast Argentina), LA-PLATA (La Plata River basin), and SE-BR (Southeastern Brazilian coast). The diagram highlights the cyclogenesis frequency and seasonal patterns in each region, with a visual scale indicating activity levels from more active to less active.

2.2.2 Genesis mechanisms

The majority of systems in SESA region are extratropical (Marrafon et al., 2022), thus baroclinic instability serves as the primary genesis mechanism across all regions, as discussed in Section 2.1.3. However, each region is also influenced by secondary mechanisms. Notably, all regions lie on the lee side of the Andes, where baroclinic development of troughs crossing the mountain range can prompt surface cyclogenesis (Gan and Rao, 1994; Vera et al., 2002; Hoskins and Hodges, 2005; Gramcianinov et al., 2019). Additionally, downstream development, marked by system decay on the Andes' upslope and regeneration on the downslope facilitated by vortex stretching over the mountain barrier, is observed (Hoskins and Hodges, 2005).

Subsequent analyses by Gramcianinov et al. (2019) and Crespo et al. (2021) delve into the specific genesis mechanisms for each cyclogenesis region. Their findings, synthesized in this section, compare summer and winter mechanisms, as transitional seasons typically exhibit intermediate characteristics (Gan and Rao, 1991; Hoskins and Hodges, 2005; Gramcianinov et al., 2019; Crespo et al., 2021).

In both seasons, cyclones in ARG region tend to follow a traditional baroclinic development pathway, heavily influenced by low level cold advection (Gramcianinov et al., 2019). This advection is crucial in reducing static stability, due to the contrast between the warmer surface and cold air aloft, thereby facilitating cyclogenesis. The cyclogenesis position relative to the jet stream provides upper-level support, either at the poleward exit during summer or the equatorward entrance during winter (Crespo et al., 2021). During summer, a slightly more baroclinic environment and more pronounced potential vorticity anomalies promote conditions favorable for ascending vertical movements (Crespo et al., 2021).

Cyclone development in the LA-PLATA region is initially driven by moisture transport from the South American low-level jet on the eastern slope of the Andes and from the South Atlantic Subtropical High towards the southeastern coast (Gramcianinov et al., 2019). This transport feeds cyclone development with warm, moist air, promoting low-level instability. Furthermore, cyclogenesis in this region is influenced by potential vorticity anomalies in both summer and winter (Crespo et al., 2021). The area is positioned beneath the equatorial entrance of a jet streak in both seasons, with a slightly more pronounced baroclinic environment in winter (Crespo et al., 2021).

During summer, cyclogenesis in the SE-BR region is significantly influenced by the transport of warm and moist air from the tropics, associated with the South Atlantic Convergence Zone (SACZ) (Gramcianinov et al., 2019). This process contributes to cyclogenesis through diabatic heating and convective processes. In winter, upper-level forcing becomes more prominent, with baroclinic conditions intensified by the presence of strong temperature gradients and jet stream dynamics (Gramcianinov et al., 2019). Moreover, during summer, cyclogenesis occurs in a more barotropic environment, with the jet stream significantly displaced from the genesis region, and is highly influenced by high-level potential vorticity anomalies (Crespo et al., 2021). Conversely, in winter, cyclogenesis occurs beneath the equatorial entrance of a jet streak in a more baroclinic environment compared to summer, influenced by low-level potential vorticity anomalies (Crespo et al., 2021).

2.2.3 Subtropical cyclones

It was only after Hart (2003) work that the scientific community started to take a closer look to subtropical cyclones. It wasn't until about 20 years ago that the first detailed climatology for subtropical cyclones in the South Atlantic was conducted by Evans and Hart (2003). This study uncovered an average occurrence of roughly one subtropical cyclone per year in the region, with a relatively uniform distribution across seasons. Notably, subtropical cyclogenesis was found to occur in diverse environments: genesis in the open ocean primarily involves Rossby wave breaking, similar to systems in the North Atlantic, whereas coastal genesis is often related to lee cyclogenesis, influenced by the warmer sea surface temperatures of the Brazilian Current, which create conducive conditions for subtropical cyclone formation.

More recently, Gozzo et al. (2014) introduced modifications to the criteria used by Evans and Hart (2003), aiming to capture weaker and shallower systems in their analysis. This adjustment led to the identification of an average of 7 cyclones per year, a significant increase from the findings of the previous study. Gozzo et al. (2014) emphasized the subtropical cyclones' lower traveled distance and displacement speed compared to their extratropical counterparts, allowing them more time to interact with the unstable conditions that facilitated their genesis and to exert greater impact on the South American coastal zone.

Moreover, Gozzo et al. (2014) noted distinctions in seasonal activity, with a peak during summer but stronger systems occurring in autumn. The Southeastern Brazil region (SE-BR) emerged as the predominant genesis area, with over a third of the cyclones developing there exhibiting hybrid characteristics. These systems typically originate from upper-level potential vorticity anomalies and divergence within a low-shear environment. At lower levels, warm and moist air advection, primarily from the subtropical high, is crucial for their formation. During summer, an additional moisture source from the tropics is also significant. Also, the authors used numerical simulation for demonstrating the importance of local latent heat fluxes for the systems develoment.

Gozzo et al. (2017) reinforced the findings of Gozzo et al. (2014), confirming the role of moisture fluxes in the formation of subtropical cyclones in the SE-BR region. They highlighted that moisture transport from the subtropical high is particularly crucial during the summer months when it shifts closer to the Brazilian southeastern coast. The reduced number of genesis events observed in the winter can be attributed to the diminished strength of this moisture transport. In contrast, during autumn, transient high-pressure systems serve as the primary source of moisture. Moreover, through numerical simulations, the authors demonstrated the significance of local latent heat fluxes in the development of these systems.

Subtropical cyclones in the South Atlantic remain an area ripe for exploration due to their relatively sparse coverage in scientific literature. From the limited climatologies available, and the few study cases (Reboita et al., 2018, 2022; Dias Pinto and Rocha, 2011, e.g.) it is evident that the formation of these systems is closely linked to Rossby wave breaking and are fueled by both local and non-local latent heat fluxes. However, the door remains open for more comprehensive studies to explore the their dynamics, climatological impacts, and the potential influence of broader atmospheric and oceanic processes on their formation.

2.2.4 Tropical cyclones

Historically, it was believed that the SESA was not conducive to Tropical Cyclone formation due to insufficiently high sea-surface temperatures and relatively strong vertical wind shear, a perspective dating back to Gray (1968), which identified the South Atlantic as the sole oceanic basin without such systems. This view was upended by Hurricane Catarina in 2004, the first recorded hurricane in the South Atlantic, challenging previous assumptions despite some evidence of weak tropical cyclones in the region before the satellite era (da Silva Dias et al., 2004).

Catarina, which originated from an extratropical system near the southeastern Brazilian coast, underwent a tropical transition and made landfall in Southern Brazil (Pezza and Simmonds, 2005). The system's trajectory and development were significantly influenced by unique environmental conditions, including a dipole-blocking pattern in the upper atmosphere, guiding the system back toward Brazil over relatively cool sea surface temperatures (SSTs) of around 25°C (McTaggart-Cowan et al., 2006). This development over cooler SSTs was facilitated by a unique combination of extreme blocking conditions, low wind shear favored by an extreme positive phase of the Southern Annular Mode (Pezza and Simmonds, 2005; Pezza et al., 2009), and latent heat release from air-sea interactions. Strong interactions with sub-superficial warm waters by Ekman pumping led to the upwelling of isotherms and mixed layer waters, allowing for a significant air-sea temperature gradient and vigorous heat exchange between the ocean and atmosphere, fueling the system through latent heat release (Vianna et al., 2010; Pereira Filho et al., 2010).

Hurricane Catarina, while a landmark event, did not originate from a purely tropical process; it was a baroclinic cyclone that underwent tropical transition. This distinction was pivotal until the emergence of a system near Brazil's Northeast oceanic region in 2019, reported as the first instance of pure tropical cyclogenesis in the South Atlantic. This system, named Iba, marked a significant departure from previous understandings of cyclonic activity in the region (Reboita et al., 2021). Additionally, research on subtropical cyclone Anita in March 2010 suggested its potential for tropical transition under warmer sea surface conditions and without interference from a neighboring extratropical cyclone (Dias Pinto and Rocha, 2011; Reboita et al., 2019). In March 2024, another system named Akará, originating near Southeastern Brazil and featuring eye-like characteristics and a symmetric form, ignited discussions regarding its potential classification as a tropical cyclone, although a detailed examination of its characteristics is pending.

The sporadic nature of these systems in the SESA region precludes the formation of a comprehensive tropical cyclone climatology. While there is some conjecture about the influence of climate change on the emergence of these systems (Pezza and Simmonds, 2005; McTaggart-Cowan et al., 2006; Pezza et al., 2009; Pereira Filho et al., 2010, e.g.,), establishing a direct connection between recent tropical cyclone occurrences in SESA and global climatic shifts remains elusive. The rarity of such events continues to challenge researchers, suggesting a complex interaction between regional climatic conditions and broader atmospheric patterns influenced by climate change.

2.3 Life cycle of extratropical cyclones: objective classification procedures

This section explores lifecycle and classification procedures for extratropical cyclones, building upon conceptual models and evolution patterns discussed in Sections 2.1.2 and 2.1.3. These models, derived from case studies and numerical simulations, seek to generalize cyclone development phases due to the absence of standardized methods for analyzing distinct lifecycle stages across extensive datasets. Herein, we introduce an automated approach for detecting the lifecycle of cyclones, thereby advancing the discussion on objective classification methodologies for these atmospheric phenomena.

The Polar Front Theory, as detailed by Bjerknes and Solberg (1922), was among the first to describe the lifecycle of extratropical cyclones, delineating distinct phases based on structural transformations and large-scale dynamics. Nonetheless, Shapiro and Keyser (1990) later argued that not all cyclones adhere strictly to the progression outlined by Bjerknes, proposing an alternative model that complements the original theory. These developmental models, including their respective stages, are elaborated in Section 2.1.2 and illustrated in Figure 2.4. While these descriptions offer detailed insights into the structural changes cyclones undergo, they fall short of directly associating each phase with specific atmospheric variables in a way that allows for algorithmic detection and statistical and/or spatial analysis.

Whittaker and Horn (1984) conducted one of the earliest cyclone climatology studies, identifying cyclogenesis regions based on the formation of the first closed isobar. This definition has been widely used since (Gramcianinov et al., 2019; Trigo, 2006; Hoskins and Hodges, 2005; Simmonds and Keay, 2000, e.g). Whittaker and Horn (1984) also defined cyclone intensification as the rate of sea level pressure deepening, a definition echoed and expanded upon by later studies through metrics like relative vorticity growth rate (Grise et al., 2013; Gramcianinov et al., 2019; Hoskins and Hodges, 2005) and the baroclinic Eady growth rate (Pinto et al., 2005). However, Whittaker's study lacked a comprehensive method for classifying cyclone evolution.

A classification of the developmental phases throughout the life cycle of cyclones was conducted by Evans and Hart (2003), with a particular focus on tropical cyclones undergoing extratropical transition. This study explored the structural evolution of such systems, employing a classification framework grounded in the environmental parameters outlined by Hart (2003). The authors partitioned the life cycle of the cyclones into two main phases: one preceding and the other following the peak intensity of the tropical cyclone. This demarcation enabled a detailed analysis of the transformation these cyclones undergo from their genesis as tropical entities to their eventual extratropical characteristics.

Gray and Dacre (2006) implemented the classification scheme originally proposed by Deveson et al. (2002), as detailed in Section 2.1.3, to study the climatology of Northern Atlantic extratropical cyclones. Their analysis focused on the separation between the upper-level trough and the lower-level cyclone throughout the cyclones' intensification periods, which were identified when the cyclones' central relative vorticity surpassed a specified threshold. While this approach proved beneficial for classification purposes, it overlooked the exploration of dynamical forcing during the development of cyclones. Furthermore, the rationale behind the selected threshold value, including its potential applicability across various scenarios, remained unexplored.

Building upon the foundation laid by Gray and Dacre (2006), Dacre and Gray (2009) delved into the environmental forces influencing the evolution of different types of cyclones. To achieve a granular understanding of variations throughout the cyclones' life cycle, they segmented the cycle at the juncture of maximum relative vorticity. This segmentation delineated the period leading up to this juncture as the intensification stage and the subsequent period as the decaying stage. Additionally, by categorizing cyclones based on their overall lifespan, the study facilitated the identification of specific areas prone to cyclone intensification and the environmental characteristics predominant in those regions.

Rudeva and Gulev (2007) delved into the study of changes in the radius of cyclones throughout their life cycle, introducing the concept of "nondimensional cyclone lifetime." This methodology facilitates the comparison of different stages of cyclone development by normalizing their lifespan to a uniform scale, achieved by dividing the current time step within the system's life cycle by its total duration. Similar apporaches were employed by Booth et al. (2018) and Schemm et al. (2018). Specifically, Booth et al. (2018) focused on analyzing precipitation rates through the cyclone life cycle, identifying the cyclones' peak dynamical strength with the point of maximum relative vorticity. Concurrently, Schemm et al. (2018) applied normalization to the cyclone life cycles using the duration from genesis to lysis, thereby examining the periods when the systems were associated with frontal structures.

Trigo (2006) explored the spatial distribution of cyclogenesis (i.e., the initial detection point of each low-pressure system), cyclolysis (the final detected position), and the locations where these systems attained their minimum central pressure. Similarly, Bengtsson et al. (2009), albeit not explicitly defining developmental stages, observed distinguishable phases centered around the maximum intensity of the system, characterized as the period when maximum central relative vorticity is reached. Meanwhile, Azad and Sorteberg (2014a,b) dissected the cyclone life cycle into distinct stages, identifying the mature phase as the period during which geostrophic vorticity experiences its most rapid increase, with the incipient stage occurring beforehand. Moreover, they categorized the life cycle of a cyclone based on the maximum geostrophic vorticity attained; the time leading up to this peak is labeled as the intensification stage, while the subsequent period is known as the decaying stage.

The diverse methodologies highlighted in the literature offer a range of objective criteria for delineating the lifecycle of extratropical cyclones, each linked to the temporal dynamics of specific atmospheric variables. Commonly, cyclone genesis is identified at the algorithm's first detection, with intensification and decay phases typically defined by changes in central pressure or, when using relative vorticity for tracking, by the increase (intensification) or decrease (decay) of vorticity in the Northern Hemisphere. The peak of the system's intensity is often marked as the point of maturity, while lysis is recognized at the algorithm's final detection of the system. A schematic illustration of this lifecycle, emphasizing the use of relative vorticity at the 850 hPa isobaric level (ζ_{850}) for cyclone detection, is depicted in Figure 2.14.

Despite these advancements, several limitations persist in current approaches. First, the initial phase of cyclone development, where the system is present but not yet fully formed, is often overlooked. In such instances, a cyclone may exhibit closed central relative vorticity without corresponding closed isobars at sea level pressure (Sinclair, 1995, e.g.). Second, defining cyclone maturity as merely the point of maximum intensity overlooks the broader period during which atmospheric dynamics illustrates the cyclone's evolution. Finally, characterizing all stages between genesis and maturity as intensification, and those between maturity and lysis as decay, presupposes a singular, linear progression of these stages. This assumption fails to account for the potential complexity of cyclone lifecycle

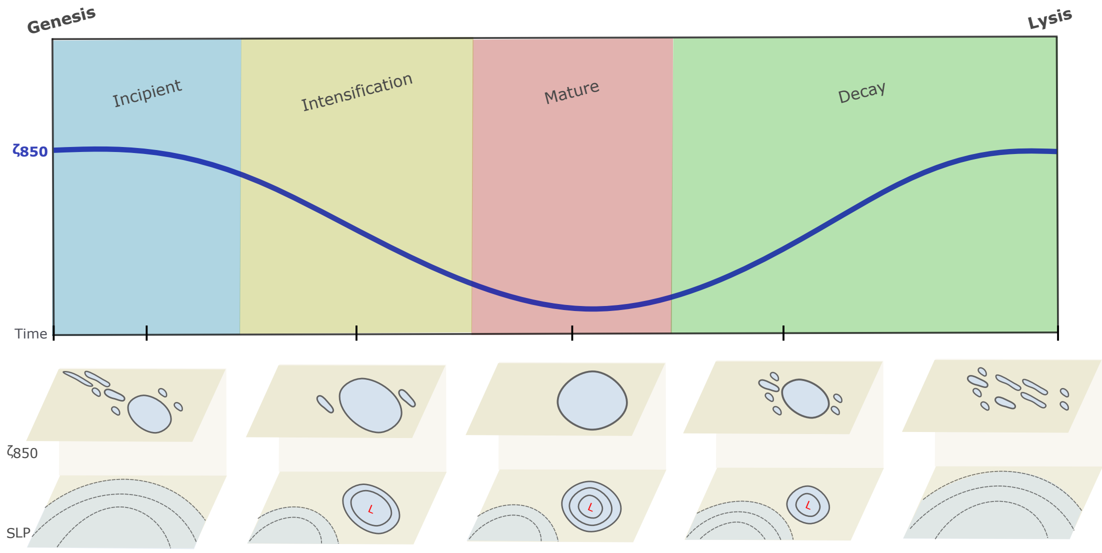

Figure 2.14: Schematic representation of an extratropical cyclone's life cycle, depicted through the relative vorticity field at the 850 hPa isobaric level (ζ_{850}). The central figure displays the temporal progression of central ζ_{850} at the cyclone's core across various phases. The bottom figures illustrate the evolution of the ζ_{850} field and sea level pressure (SLP) spatial distributions during each phase.

stages, including the possibility of multiple intensification and decay phases.

The ability to discern the distinct life cycle phases of cyclones is crucial for several reasons. As highlighted in Section 2.2, most climatologies currently focus on either the entirety of a cyclone's life cycle or specific points, such as its genesis or lysis. Enhanced techniques for dissecting a cyclone's life cycle could unlock the potential for more granular analyses of the processes and environmental dynamics associated with different stages of cyclone development. For example, while the initial baroclinicity associated with extratropical cyclones is well-documented, the environmental shifts that trigger their cessation of intensification remain less understood. Case studies have shed light on these aspects, but comprehensive testing under climatological conditions is yet to be conducted.

By identifying the environmental conditions pertinent to various stages of cyclone development, researchers can leverage climate change projections to assess potential future shifts in these conditions. Moreover, given the absence of a universally recognized conceptual model for tropical cyclone development, detailed climatological analyses of environmental parameters across distinct life cycle phases could offer critical insights toward establishing such a model. Thus, the potential applications of a refined procedure for analyzing cyclone life cycle phases are vast, limited only by the creativity and curiosity of the research community. Such advancements would not only enhance our understanding of cyclone dynamics but also improve our ability to predict and respond to these powerful weather systems in the context of a changing climate.

2.4 Atmosphere Energetics

Solar radiation serves as the primary energy source within the Earth's system. Concurrently, the atmosphere globally dissipates heat by emitting infrared radiation into space. The tilt of the Earth's axis causes a significant variation in radiative incidence between the tropical and polar regions: tropical areas receive more solar energy than they emit, creating an energy surplus, whereas polar regions experience an energy deficit, losing more energy to space than they absorb. This differential heating leads to the formation of warm air masses in tropical regions and cold air masses in polar regions. The resulting heat imbalance drives atmospheric circulation, an ongoing process attempting to balance these temperature disparities. However, this equilibrium is never fully achieved due to the constant differential heating between the tropical and polar regions (Stull, 2015).

2.4.1 Lorenz Energy Cycle: Historical Background

The Lorenz Energy Cycle, introduced by Lorenz (1955), is a framework for understanding how energy is distributed and transformed within the atmosphere. This framework offers insights into the general circulation that shapes the dynamic and thermodynamic structures of the atmosphere, influencing atmospheric flows and the transport of heat, moisture, and angular momentum. In his groundbreaking work, Lorenz delineated a method to analyze atmospheric energetics by focusing on two primary forms of energy: kinetic energy (K) and available potential energy (APE), each further divided into zonal and eddy (turbulent) components. This section explores these energy forms and their interactions.

Lorenz argued that the total potential energy (P) of the atmosphere does not effectively represent the energy available for conversion into K to drive global circulation. To illustrate this concept, Lorenz proposed a thought experiment: Imagine the atmosphere is uniformly horizontally stratified; in such a scenario, despite the presence of P, the lack of horizontal gradients precludes air mass movement, resulting in no generation of K (Figure 2.15a). However, if part of the atmosphere is heated, it triggers vertical upward movements, establishing pressure gradients and disrupting the horizontal stratification (Figure 2.15b). Conversely, cooling in a region induces similar effects but with vertical downward movements (Figure 2.15c). Both scenarios alter the P of the system, converting it into K. Yet, in the first case, P increases, while in the second, it decreases; that is, both increases and decreases of P are responsible for making energy available for atmospheric circulation.

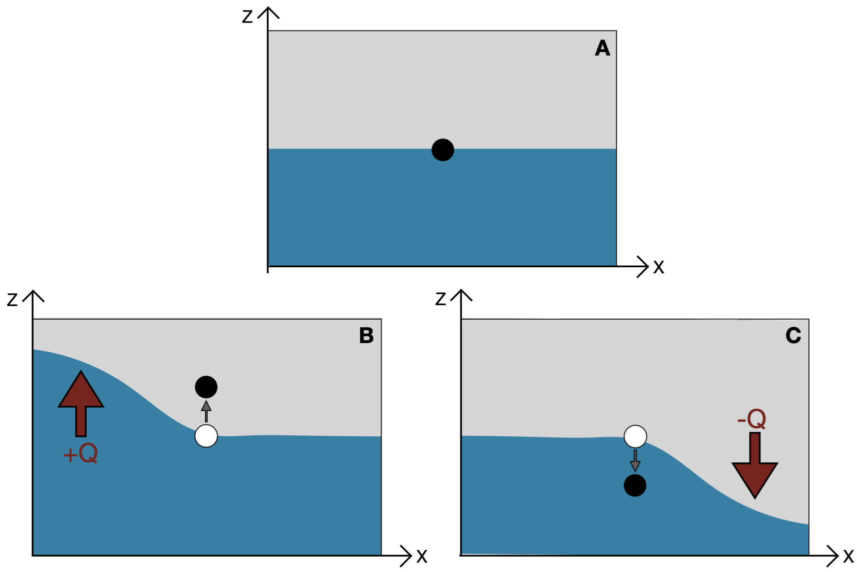

Figure 2.15: Mental experiment proposed by Lorenz (1955) to illustrate the relationship between total P and K, depicted through a two-layer atmospheric model: (A) Initially horizontally stratified atmosphere. (B) Perturbation caused by localized heating (+Q) leading to vertical upward movements. (C) Similar perturbation caused by cooling (-Q) resulting in vertical downward movements. Black circles represent the atmosphere's center of mass post-perturbation, and white circles indicate the center of mass prior to perturbation.

The concept of Available Potential Energy (APE) was initially proposed by Margules (1903), who was interested in the processes that generate kinetic energy (K) in storms (Marquet, 2017). To understand this concept, we can start from the same situation proposed by Lorenz (1955), where differential heating results in ascending movements and a heterogeneous distribution of mass in the atmosphere (Figure 2.16a). In this case, the resulting pressure gradients cause acceleration of the wind field (Figure 2.16b), redistributing the mass in the atmosphere. Assuming this flow is adiabatic, the final result is a horizontally stratified atmosphere (Figure 2.16c). In the first step, both forms of potential energy (total and available) are at their maximum. With the redistribution of mass, there is an increase in K, while the total and available potential energy decreases. In the final stage, P is minimal, yet not zero, while the APE is zero. Thus, APE can be defined as the amount of potential energy available for conversion into K under an adiabatic distribution of mass.

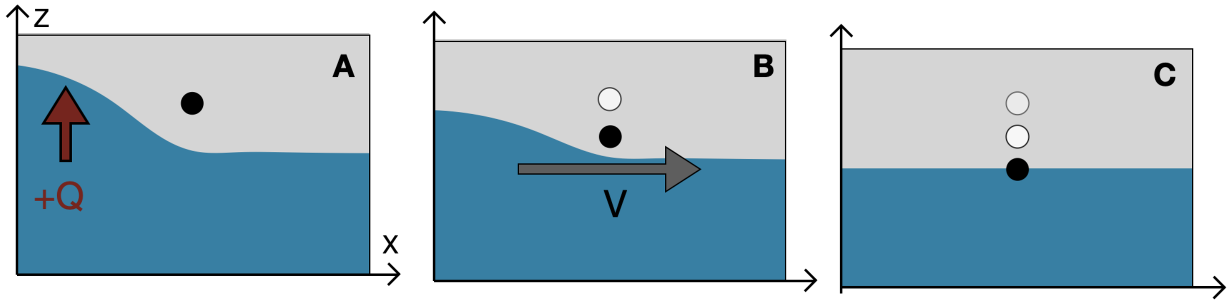

Figure 2.16: Depiction of Available Potential Energy (APE) transformations in response to atmospheric heating and cooling. (A) Initial state with differential heating causing heterogeneous mass distribution. (B) Redistribution of mass via wind fields leading to homogenization. (C) Final state of horizontal atmospheric stratification. Black circles indicate the center of mass at each stage, with white circles showing previous positions.

According to Lorenz (1955), APE serves as the primary source of K in the atmosphere, fundamentally driving the general circulation. While APE and K dominantly shape atmospheric dynamics, Lorenz acknowledged that diabatic processes and friction also play critical roles, though these elements were less detailed in his work due to their complex nature and the challenges associated with their quantification. In his theoretical framework, Lorenz treated the atmosphere as a closed system, distinguishing between the zonal and eddy (turbulent) components of APE and K to clarify the energetics involved in atmospheric processes.

This distinction is crucial as it aligns with earlier observations by Starr (1953), who emphasized the significance of eddies in maintaining atmospheric circulation, particularly their role in transferring K from turbulent to zonal flows. This perspective challenged earlier assumptions and highlighted the necessity of including eddy dynamics in any comprehensive atmospheric circulation theory. Subsequent research by Wiin-Nielsen et al. (1963) demonstrated the importance of eddies in global heat and momentum transport, illustrating how different wave numbers contribute to these processes. Through these insights, Lorenz's separation of energy components facilitates a deeper understanding of how meteorological systems, such as cyclones, develop and influence broader atmospheric circulation patterns.

The energy cycle can be represented by the following equations, which represent the energy balance for each component of the cycle:

$$\frac{\partial A_Z}{\partial t} = -C_Z - C_A + G_Z \tag{2.6}$$
$$\frac{\partial A_E}{\partial t} = -C_E + C_A + G_E \tag{2.7}$$
$$\frac{\partial K_Z}{\partial t} = C_Z - C_K - D_Z \tag{2.8}$$
$$\frac{\partial K_E}{\partial t} = C_E + C_K - D_E \tag{2.9}$$

In these equations, available potential energy (APE) is divided into zonal (A_Z) and eddy (A_E) components, as is kinetic energy (K_Z and K_E, respectively). The transformations between these forms of energy are denoted by C, with subscripts Z and E for conversions between zonal and eddy forms, and A and K indicating conversions between APE and kinetic energy, respectively. Thus, C_A represents the conversion between A_Z and A_E, C_E denotes the conversion from A_E to K_E, C_K signifies the transformation from K_E to K_Z, and C_Z describes the conversion from A_Z to K_Z. Generation of APE and dissipation of kinetic energy are indicated by G and D, with G_Z and G_E marking the generation of A_Z and A_E, and D_Z and D_E representing the dissipation of K_Z and K_E, respectively. Full mathematical formulations for these processes are discussed in Section 2.4.2.

After the seminal work by Lorenz (1955) on the global energy cycle, numerous subsequent studies aimed to quantify this cycle, primarily focusing on the Northern Hemisphere due to observational constraints at the time (Starr, 1959; Saltzman and Fleisher, 1961; Holopainen, 1964; Jensen, 1961; Brown Jr, 1964; Wiin-Nielsen, 1959, e.g.). Oort (1964) synthesized these results to depict the annual energy cycle of the Northern Hemisphere. He innovatively categorized the energy analysis into distinct domains: the spatial domain, where variables are analyzed based on spatial averages, aiding in the understanding of large-scale zonal patterns such as jet streams and westerlies; the temporal domain, focusing on averages and deviations over time, which facilitates insights into long-term trends and transient disturbances; and the mixed space-time domain, which offers an integrated perspective on how average states and disturbances, both transient and stationary, interact and are sustained. Oort noted that while there was considerable focus on spatial domain analyses, studies addressing the mixed domain were scarce, and those considering the temporal domain were virtually absent.

From these estimates, Oort (1964) presented a diagram that visually encapsulates the energy cycle (Figure 2.17). This diagram illustrates the generation, conversion, and dissipation of different energy forms, providing a dynamic overview in a graphical format. Notably, the diagram allows for straightforward comparisons of diverse study results. It is important to mention, as Oort (1964) did, that friction terms are typically calculated as residuals due to the challenges in direct computation, balancing the zonal and turbulent terms of kinetic energy.

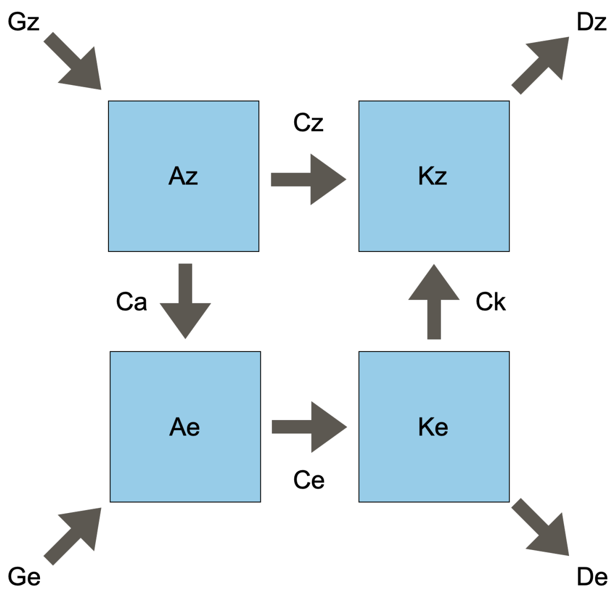

Figure 2.17: Representation of the energy cycle as formulated by Lorenz (1955) and schematized by Oort (1964). This diagram displays the interplay among the four forms of energy (zonal and turbulent terms of K and APE), illustrating their conversions, generation, and dissipation.

As previously mentioned, the formulation proposed by Lorenz (1955) estimates the energetics of the atmosphere assuming a closed system, that is, without energy exchanges at the boundaries. The first study to consider energetics for an open system was by Reed et al. (1963), which analyzed a sudden stratospheric warming event in the Northern Hemisphere. This study treated the stratosphere as an open system, permitting energy exchanges with other atmospheric layers, such as the troposphere. Building on this, Muench (1965), who was interested in stratospheric dynamics, refined Lorenz (1955)'s theory and proposed a new representation of the energy cycle.

Muench's model adds boundary flow terms (BA_Z, BA_E, BK_Z, and BK_E) to the original Lorenz equations, representing respectively the zonal and eddy flows of APE and K across the system boundaries (Figure 2.18). The updated energy balance equations are:

$$\frac{\partial A_Z}{\partial t} = BA_Z - C_Z - C_A + G_Z \tag{2.10}$$
$$\frac{\partial A_E}{\partial t} = BA_E - C_E + C_A + G_E \tag{2.11}$$
$$\frac{\partial K_Z}{\partial t} = BK_Z + C_Z - C_K + B\Phi_Z - D_Z \tag{2.12}$$
$$\frac{\partial K_E}{\partial t} = BK_E + C_E + C_K + B\Phi_E - D_E \tag{2.13}$$

Where BA_Z, BA_E, BK_Z, and BK_E represent, respectively, the flows of zonal and eddy APE and K across the boundaries. The terms $B\Phi_Z$ and $B\Phi_E$ are represented together with the terms C_Z and C_E, respectively, because both arise from the same process of deriving the balances of K_Z and K_E. Muench (1965) recognizes the difficulty in interpreting the terms $B\Phi_Z$ and $B\Phi_E$, indicating that they are related to the flow of kinetic energy towards lower altitudes, representing the emergence of kinetic energy at the boundaries of the computational domain.

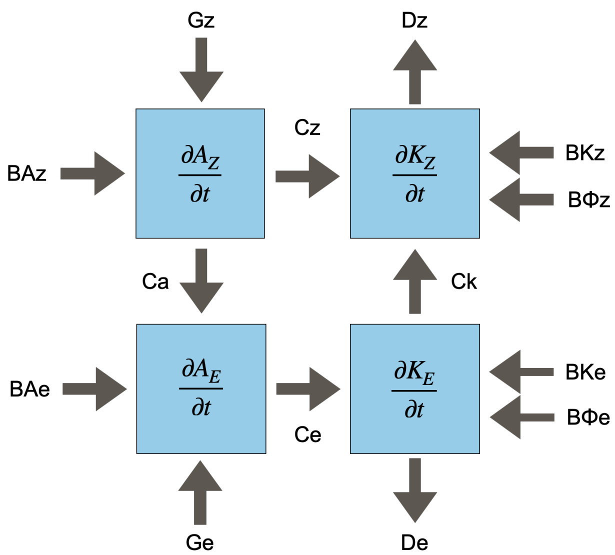

Figure 2.18: Energy cycle as formulated by Lorenz (1955) and updated by Muench (1965). This diagram includes additional terms representing energy flows across boundaries, illustrating both the local derivatives of the zonal and eddy partitions of APE and K and the interactions at the system edges.

Although Muench's model considers boundary flows, his domain was partially open, extending up to the polar regions and encompassing the entire Northern Hemisphere longitudinally, with the only boundary at the southern part of the domain at 30°N. The notion of a fully regional energy cycle was later approached by Smith (1969), who aimed to assess the contribution of a limited region to global energetics. Smith clarified that while his work presented a framework for regional analysis, an exact computation of local energetics was outside its scope, and his model did not differentiate between zonal and eddy components of APE and K.

Parallel to the work by Smith (1969), Johnson (1970), following the theoretical framework proposed by Dutton and Johnson (1967), introduced a semi-Lagrangian framework for analyzing the energy cycle of limited areas. In this formulation, the delineated area for performing energetic calculations moves with the meteorological system of interest, spanning N fixed regions that shift in space. This analysis highlights that global Available Potential Energy (APE) is the aggregate of all possible open atmospheric regions, plus a term representing the thermodynamic contrast among these regions. It's crucial to note that Smith (1969) and Dutton and Johnson (1967) argued that the APE of a limited region should be viewed as its contribution to the global energetics rather than a standalone quantity. This perspective stems from the interconnected nature of the atmosphere, where local and global energetics are mutually influential.

Dutton and Johnson (1967) also critiqued Lorenz (1955)'s formulation, pointing out its underestimation of APE, particularly during the winter months. The alternative set of equations introduced by Johnson (1970), which utilizes isentropic coordinates, however, included simplifications that were seen as limitations by Vincent and Chang (1973), such as neglecting the impact of diabatic heating, rendering it impractical for diagnostic applications. Following this rationale, Vincent and Chang (1973) developed a system of equations in isobaric coordinates that account for the balances of APE and Kinetic Energy (K) in an open atmospheric system from a semi-Lagrangian perspective.

This formulation partitions APE into the reference state APE of the region and two components representing barotropic and baroclinic contributions to the APE of the delineated area. The balance equations for APE now included terms for boundary movement in the semi-Lagrangian frame and the advection of air masses with varying properties across these boundaries. This formulation was first applied by Edmon and Vincent (1979) in an energy cycle analysis of Hurricane Carmen (1974). Building on this, Brennan and Vincent (1980) adapted Vincent's approach to incorporate zonal and eddy components of APE and K, marking the first instance of such a detailed and realistic equation set being applied to a limited are within the troposphere. However, Brennan and Vincent (1980) utilized a traditional Eulerian approach for their energy analysis.

Furthermore, Brennan and Vincent (1980) reinterpreted the boundary terms $B\Phi_Z$ and $B\Phi_E$ as the work done by zonal and meridional wind components against atmospheric pressure at the computational domain boundaries. However, they noted that these terms, as calculated, were unrealistically large due to minor errors in the geopotential height field, which could escalate in major errors and significantly skew the results. Consequently, these terms were combined with the dissipation terms (D_Z and D_E) and treated as residuals in the balance equations for K_Z and K_E, resulting in new terms RK_Z and RK_E. This approach and the updated energy cycle are depicted in Figure 2.19.

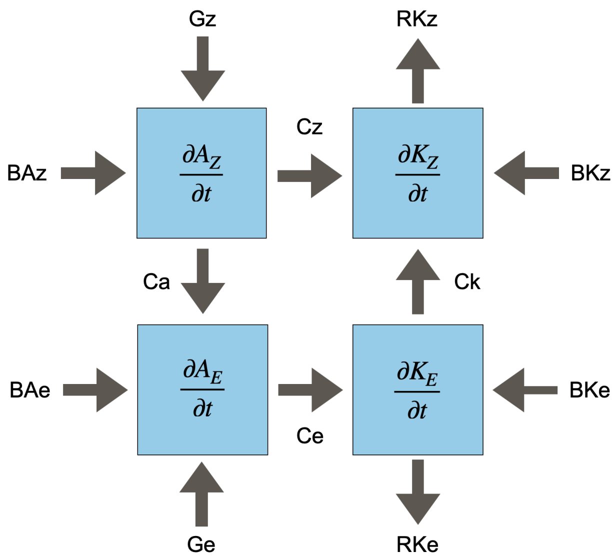

Figure 2.19: Updated energy cycle as reformulated by Brennan and Vincent (1980). This diagram includes the integrated terms for boundary energy flows ($B\Phi_Z$ and $B\Phi_E$) merged with dissipation processes (D_Z and D_E), represented as residual terms RK_Z and RK_E.

The modified energy balance equations are as follows:

$$\frac{\partial A_Z}{\partial t} = -C_A - C_Z + G_Z + BA_Z \tag{2.14}$$

$$\frac{\partial A_E}{\partial t} = C_A - C_E + G_E + BA_E \tag{2.15}$$

$$\frac{\partial K_Z}{\partial t} = C_K + C_Z + BK_Z + RK_Z \tag{2.16}$$

$$\frac{\partial K_E}{\partial t} = -C_K + C_E + BK_E + RK_E \tag{2.17}$$

And the residual terms are defined as:

$$RK_Z = B\Phi_Z + D_Z \tag{2.18}$$

$$RK_E = B\Phi_E + D_E \tag{2.19}$$

Robertson and Smith (1983) adapted the formulation presented by Brennan and Vincent (1980) for limited area domains, particularly revising the term A_E. Building upon the framework of APE for limited domains outlined by Smith et al. (1977), Robertson integrates the first law of thermodynamics into the Eulerian derivatives of the APE and A_Z formulations. This results in a significantly different balance equation for A_E, introducing a novel term associated with variations in the reference pressure field, which alters the computation of the conversion term C_A. This approach was driven by the goal of evaluating, through numerical modeling, the influence of moist processes on the energetics of extratropical cyclones. However, the adaptation necessitated computations over isentropic coordinates, introducing complexities in the numerical implementation.

In an effort to analyze the energetics of cyclogenesis in the Gulf of Genoa within the Mediterranean Sea, Michaelides (1987) advanced the energy cycle formulation further. Echoing concerns from Brennan and Vincent (1980) regarding unrealistic results for the terms $B\Phi_Z$ and $B\Phi_E$, Michaelides introduced additional residual terms RK_Z and RK_E, and a correction factor (ϵ) to account for numerical errors in the estimation of these terms, as shown in the equations and Figure 2.20. The modified set of equations is as follows:

$$\frac{\partial A_Z}{\partial t} = C_K - C_A + BA_Z + \Delta G_Z \tag{2.20}$$

$$\frac{\partial A_E}{\partial t} = C_A - C_E + BA_E + \Delta G_E \tag{2.21}$$

$$\frac{\partial K_Z}{\partial t} = C_K - C_Z + BK_Z - \Delta R_Z \tag{2.22}$$

$$\frac{\partial K_E}{\partial t} = C_E - C_K + BK_E - \Delta R_E \tag{2.23}$$

Where the residual terms are defined as:

$$\Delta R_Z = B\Phi_Z - D_Z + \epsilon_{KZ} \tag{2.24}$$

$$\Delta R_E = B\Phi_E - D_E + \epsilon_{KE} \tag{2.25}$$

$$\Delta G_Z = G_Z + \epsilon_{GZ} \tag{2.26}$$

$$\Delta G_E = G_E + \epsilon_{GE} \tag{2.27}$$

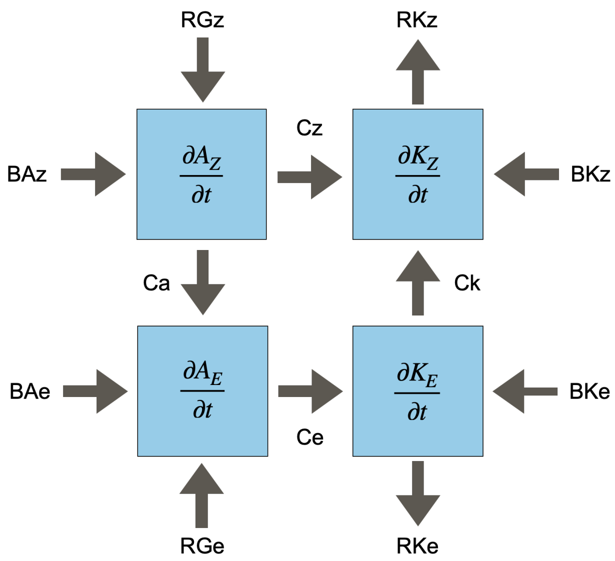

Figure 2.20: Refined depiction of the energy cycle incorporating modifications by Michaelides (1987). This representation includes error correction terms within the residual balances, addressing previous challenges with the quantification of boundary terms and dissipation factors.

In Michaelides et al. (1999), the author extends the energetic formulations presented in Michaelides (1987), exploring calculations for limited areas using both Eulerian and semi-Lagrangian reference frames. This study evaluates the energy cycle during a cyclogenesis event in the Mediterranean from these two perspectives, providing a nuanced discussion on the methodological implications of each. It highlights that the Eulerian approach is commonly preferred for energy analysis in limited atmospheric areas. This method necessitates defining a sufficiently large spatial domain to encapsulate all developmental stages of the system, including its movement and size changes. However, this approach has interpretative limitations; a broad spatial domain may inadvertently include adjacent synoptic circulations, thus diluting the specific energetics of the primary system under study.

Figure 2.21 illustrates this issue with a scenario akin to cyclogenesis in the coastal region of Southeast Brazil (Reboita et al., 2010; Gramcianinov et al., 2019, e.g.,). Here, the computational domain must encompass both the initial coastal genesis area and the subsequent oceanic trajectory of the cyclone. As the cyclone progresses to the ocean in its later stages, mesoscale circulations near the coast, such as updrafts due to surface heating and convection from sea breeze interactions with local topography, emerge. These processes can significantly alter the computed values of APE and K within the domain, affecting the energy conversion, boundary, dissipation, and generation terms, thereby complicating the interpretation of the cyclone's energy dynamics.

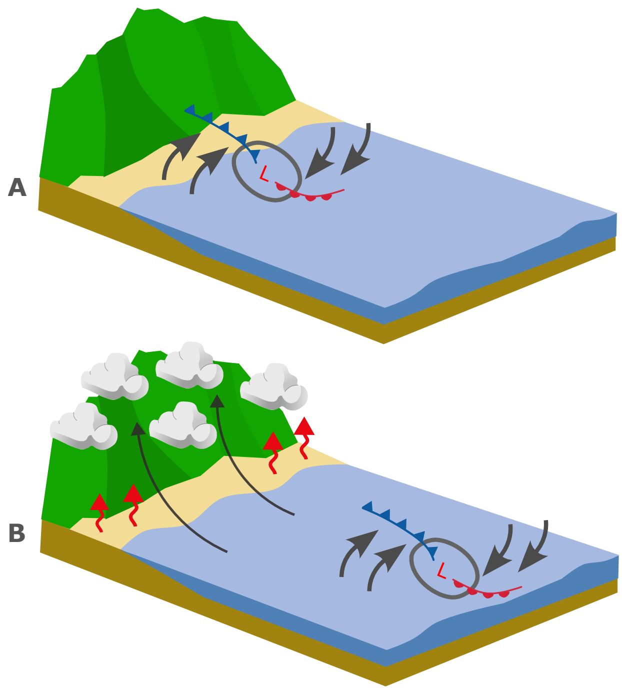

Figure 2.21: Illustration of challenges in using an Eulerian reference frame for energy cycle analysis. A) A cyclone forming near the continent, where the newly developed cyclonic system is the main meteorological feature inside the domain. B) The system is in its later oceanic phase, while meso-scale circulations develop in the coastal region, such sea-breeze and, consequently, orographic ascent over the mountain range near the coast.

Despite the inherent limitations associated with the Eulerian approach, Michaelides et al. (1999) discusses the methodological challenges of employing a purely Lagrangian framework to study extratropical cyclones. Such a study would require tracking the system in a three-dimensional space, isolated from external influences, using specific conservative variables for the encapsulated air masses. This is complicated by the diverse origins of the air masses involved in extratropical cyclones, which include both polar and tropical sources, affecting their conservative properties. Additionally, the system must be isolated from any spurious external circulations.

Consequently, Michaelides et al. (1999) advocates for a quasi-Lagrangian approach as a practical solution that minimizes the impact of neighboring circulations on the system's energy dynamics. This approach, similar to that proposed by Vincent and Chang (1973), utilizes multiple fixed domains at different temporal intervals to effectively track the cyclonic system. However, unlike Vincent and Chang (1973), Michaelides et al. (1999)'s formulation does not include terms for the displacement of computational domain boundaries. The author conducts a comparative analysis between the Eulerian and quasi-Lagrangian methods, revealing that they can yield significantly different results depending on the specific energetic terms analyzed. This highlights the complications in using the Eulerian method for comparative studies, as it can incorporate the energetic contributions of adjacent systems. Michaelides et al. (1999) concludes that the semi-Lagrangian method offers a more robust framework for analyzing the energetics of cyclonic systems. However, he notes that this approach does not allow for the local time derivatives of energy terms due to the absence of a fixed computational volume, which precludes a complete closure of the energy balance. A detailed discussion of this limitation is not provided in his study.

Several methodologies have been developed to refine diagnostic equations for atmospheric energetics, each offering unique advancements. The approach introduced by Plumb (1983) critiques traditional energy formulations for wave propagation and employs transformed Eulerian-mean equations to enhance the physical accuracy of eddy-mean flow interactions. Similarly, Marquet (1991)'s redefinition of exergy and available enthalpy provides a more complete analysis of atmospheric dynamics, accommodating factors such as static instabilities and topographical variations often oversimplified in previous models. The local APE density framework proposed by Novak and Tailleux (2018), on the other hand, introduces a positive-definite local form of potential energy, akin to kinetic energy, which can be transported, converted, and dissipated locally. Unlike the global and volume-integrated nature of Lorenz's APE, this local APE density theory adapts potential energy calculations to specific atmospheric conditions, enhancing diagnostic precision in regional climate studies. However, these methods significantly complicate the mathematical formulations, requiring increased computational resources and extending computation times, which pose substantial limitations, especially for operational purposes. Additionally, each of these frameworks introduces new challenges in the physical interpretation of the terms.

The present work adopts the formulation presented by Michaelides et al. (1999), which offers a balance between computational feasibility and physical accuracy. This framework provides results that serve as a useful diagnostic tool, facilitating an understanding of the dynamical mechanisms involved in cyclone development without requiring extensive computational resources. While the primary goal of this thesis is scientific, there is significant interest in developing an operational tool for diagnosing the energy cycle of cyclones that can be made available to the scientific community. This tool is envisioned to function similarly to the Hart phase diagrams, which are accessible online (https://moe.met.fsu.edu/cyclonephase/ecmwf/fcst/index.html) and widely used for real-time cyclone analysis. The complete mathematical formulation and physical interpretation of each term in the Lorenz Energy Cycle (LEC) are detailed in Section 2.4.2. Additionally, Section 3.3 describes the computational methods used to calculate the LEC.

2.4.2 Lorenz Energy Cycle: Mathematical expressions and physical interpretation

This section provides a detailed description of the symbols and expressions used for the calculation of the Lorenz Energy Cycle (LEC), adopting the notation from Michaelides (1987).

Firstly, we define the zonal mean of a variable X, between longitudes λ_1 and λ_2:

$$[X]_\lambda = \frac{1}{\lambda_2 - \lambda_1} \int_{\lambda_2}^{\lambda_1} X d\lambda \tag{2.28}$$

The eddy component of this variable is its deviation from the zonal mean:

$$(X)_\lambda = X - [X]_\lambda \tag{2.29}$$

The domain mean of the variable X, defined over the computational domain bounded by longitudes λ_1 and λ_2, and latitudes ϕ_1 and ϕ_2, is given by:

$$[X]_{\lambda\phi} = \frac{1}{\lambda_2 - \lambda_1} \frac{1}{\sin\phi_2 - \sin\phi_1} \int_{\lambda_2}^{\lambda_1} X cos\phi d\lambda d\phi \tag{2.30}$$

Similarly, we define the deviation of the zonal mean from the domain mean:

$$([X]_\lambda)_\phi = [X]_\lambda - [X]_{\lambda\phi} \tag{2.31}$$

From the definitions above, the four energy components used in the LEC computation are defined as follows:

$$A_Z = \int_{p_t}^{p_b} \frac{([(T)_\lambda])_\phi^2]_{\lambda\phi}}{2[\sigma]_{\lambda\phi}} dp \tag{2.32}$$

$$A_E = \int_{p_t}^{p_b} \frac{[(T)_\lambda^2]_{\lambda\phi}]}{2[\sigma]_{\lambda\phi}} dp \tag{2.33}$$

$$K_Z = \int_{p_t}^{p_b} \frac{[[u]_\lambda^2 + [v]_\lambda^2]_{\lambda\phi}}{2g} dp \tag{2.34}$$

$$K_E = \int_{p_t}^{p_b} \frac{[(u)_\lambda^2 + (v)_\lambda^2]_{\lambda\phi}}{2g} dp \tag{2.35}$$

where p is the atmospheric pressure, with subscripts b and t denoting the lower (base) and upper (top) pressure boundaries of the atmosphere, respectively. T represents temperature, g is the acceleration due to gravity, and u and v are the zonal and meridional wind components, respectively. The static stability parameter σ is defined as:

$$\sigma = \left[\frac{gT}{c_p} - \frac{pg}{R} \frac{\partial T}{\partial p} \right]_{\lambda\phi} \tag{2.36}$$

where c_p is the specific heat at constant pressure, and R is the ideal gas constant for dry air.

The APE terms A_Z and A_E are related to the situations described in Section 2.4 and showcased in Figure 2.16. For A_Z, higher values for the numerator mean greater differences in the latitudinal mean temperature, which corresponds to a greater latitudinal temperature gradient, such as the equator being hotter than the poles. Additionally, lower values for the denominator indicate a more unstable atmosphere. An unstable atmosphere can redistribute vertical motions more easily and, therefore, can produce greater gradients in the latitudinal mean temperature. The term A_E is analogous to A_Z, but in this case, the temperature gradient is longitudinal rather than zonal, caused by eddy motions. This situation indicates a higher amount of available potential energy, either zonal or eddy, which can be converted into kinetic energy, thus driving atmospheric motions.

The kinetic energy terms K_Z and K_E represent the intensity of the atmospheric motions. K_Z is proportional to the zonal mean of the sum of the wind components. Since winds from opposite directions would cancel each other out, K_Z has greater values whenever the winds in the same latitude circle have the same direction. $[u]_\lambda$ captures the large-scale east-west circulation, such as the trade winds, westerlies, and jet streams, while $[v]_\lambda$ captures the north-south circulations, such as the Hadley cell and polar cell circulations. Thus, higher values of K_Z indicate stronger mean circulations, which contribute to the overall momentum and energy of the atmospheric system. Meanwhile, $(u)_\lambda$ and $(v)_\lambda$ represent the deviations of the wind components from their mean values, capturing the smaller-scale, turbulent motions and deviations from the mean flow. These eddy motions include phenomena such as cyclones, anticyclones, and other mesoscale and synoptic-scale disturbances. Thus, higher values of K_E indicate more vigorous eddy activity, which contributes to the overall turbulence and mixing within the atmosphere.

The four conversion terms are defined as follows, integrating over the atmospheric column from the base (p_b) to the top (p_t) pressures:

$$C_Z = \int_{p_t}^{p_b} -[([T]_\lambda)_\phi([\omega]_\lambda)_\phi]_{\lambda\phi}\,\frac{R}{gp}\,dp \tag{2.37}$$

$$C_E = \int_{p_t}^{p_b} -[(T)_\lambda(\omega)_\lambda]_{\lambda\phi}\,\frac{R}{gp}\,dp \tag{2.38}$$

$$C_A = \int_{p_t}^{p_b} -\left(\frac{1}{2a\sigma}\left[(v)_\lambda(T)_\lambda\frac{\partial([T]_\lambda)_\phi}{\partial\phi}\right]_{\lambda\phi} + \frac{1}{\sigma}\left[(\omega)_\lambda(T)_\lambda\frac{\partial([T]_\lambda)_\phi}{\partial p}\right]_{\lambda\phi}\right) dp \tag{2.39}$$

$$\begin{aligned} C_K = \int_{p_t}^{p_b} \frac{1}{g}\Bigg(&\left[\frac{\cos\phi}{a}(u)_\lambda(v)_\lambda\frac{\partial}{\partial\phi}\left(\frac{[u]_\lambda}{\cos\phi}\right)\right]_{\lambda\phi} + \left[\frac{(v)_\lambda^2}{a}\frac{\partial[v]_\lambda}{\partial\phi}\right]_{\lambda\phi} \\ &+ \left[\frac{\tan\phi}{a}(u)_\lambda^2[v]_\lambda\right]_{\lambda\phi} + \left[(\omega)_\lambda(u)_\lambda\frac{\partial[u]_\lambda}{\partial p}\right]_{\lambda\phi} + \left[(\omega)_\lambda(v)_\lambda\frac{\partial[v]_\lambda}{\partial p}\right]_{\lambda\phi}\Bigg) dp \end{aligned} \tag{2.40}$$

where a is the Earth's radius and ω is the vertical velocity in isobaric coordinates.

The C_Z term (Equation 2.38) is somewhat analogous to A_Z as it is the covariance product of the temperature and vertical motions, averaged for the same latitudinal circle, where positive values mean conversion from A_Z to K_Z and vice-versa. As in the integrand we have the covariance product of the zonal deviation from the domain mean of $-T\omega$, positive values of C_Z is then related to either vertical ascent of warm air or sinking of cold air. Meanwhile, negative values of C_Z is related to ascent of air in cold regions or descent of air in warm regions. This situation is illustrated in Figure 2.22, where is represented a region with meridional gradients of temperature and vertical velocity. In this scenario, on the warmer regions as the temperature zonal deviation is positive and the ω zonal deviation is negative, the ending result is negative, while the opposite is true for the cold regions. Combining this with the negative sign and we have positive values of C_Z, i.e., conversion from A_Z to K_Z. In an opposite situation, with descending air on the warmer regions and rising air on cold regions, the covariance product would be positive and then, combining this with the negative sign, C_Z would be negative, i.e., conversion from K_Z to A_Z.

Figure 2.22 illustrates the interpretation of the term C_Z, depicting a region with meridional gradients of temperature and vertical velocity. In this scenario, in warmer regions where the temperature deviation is positive and the ω deviation is negative, the product $T\omega$ is negative. Combined with the negative sign in C_Z, this results in a positive value, indicating a conversion from A_Z to K_Z. Conversely, in colder regions, where the temperature deviation is negative and the ω deviation is positive, the product $T\omega$ is also negative, leading to a positive C_Z. In the opposite situation, with descending air in warmer regions and rising air in colder regions, the product $-T\omega$ would be positive. This, combined with the negative sign, would result in a negative C_Z, indicating a conversion from K_Z to A_Z.

The C_E term represents the conversion between the eddy forms of energy, APE (A_E) to kinetic (K_E). The C_E interpretation is similar as for C_Z, but in this case the gradients and deviations are along the longitudinal axis (x-axis) rather than the latitudinal axis (y-axis). If the axes in Figure 2.22 were swapped, it would represent a situation of positive C_E.

The C_A term (Equation 2.39) represents the energy conversion between A_Z (zonal mean available potential energy) and A_E (eddy available potential energy). Positive values indicate energy transfer from A_Z to A_E, and negative values indicate the reverse. The formulation can be split into two components, capturing how the deviations from the zonal mean of the north-south and vertical winds (for the first and second components, respectively) interact with the latitudinal temperature gradients. In the first component, we have $(v)_\lambda (T)_\lambda \frac{\partial([T]_\lambda)_\varphi}{\partial\varphi}$. Due to the minus sign in the equation, for it to contribute to C_A being positive, it has to be negative.

For understating each term contribution to C_A signal, here it is described one illustrative case, showcasing a midlatitude low-pressure system in the Southern Hemisphere, with a cold front propagating west of it and a warm front east (Figure 2.23. On the cold front region $(v)_\lambda$ is positive (northward), $(T)_\lambda$ is negative (cooler), and $\frac{\partial([T]_\lambda)_\varphi}{\partial\varphi}$ is positive (temperatures increasing with latitude). On the warm front region $(v)_\lambda$ is negative (southward), $(T)_\lambda$ is positive (warmer), and $\frac{\partial([T]_\lambda)_\varphi}{\partial\varphi}$ is positive (temperatures increasing with latitude). In both cases, $\frac{\partial([T]_\lambda)_\varphi}{\partial\varphi}$ is positive as, in the Southern Hemisphere, northerly latitudes are warmer than southerly latitudes. For the Northern Hemisphere, the same analysis can be made by inverting the sign of the meridional wind and temperature gradient, resulting in

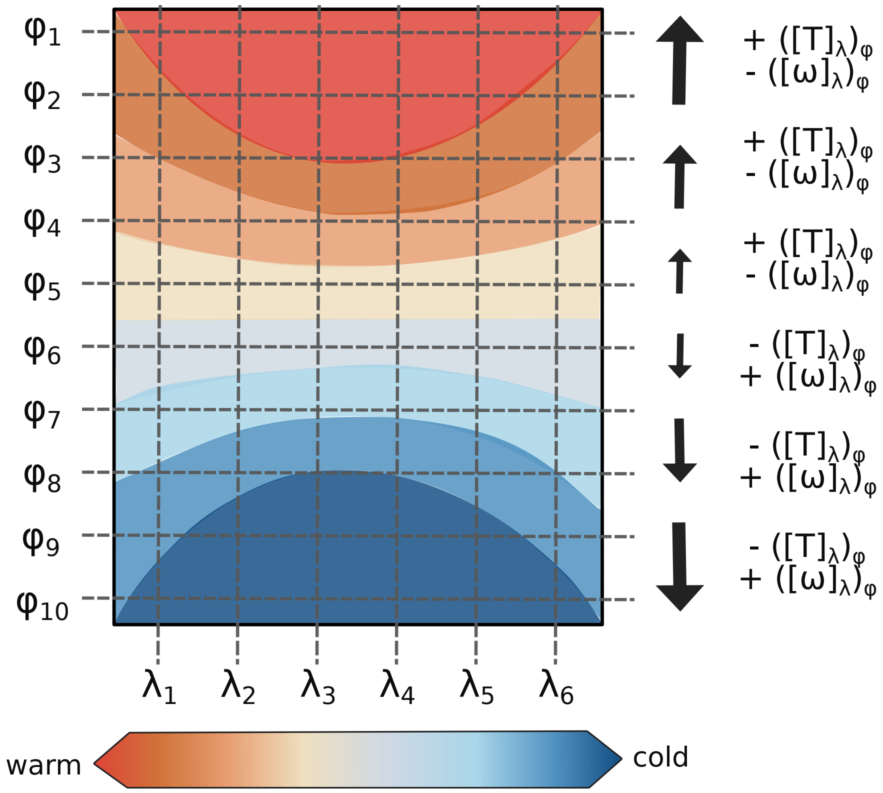

Figure 2.22: Hypothetical situation illustrating the conversion term between A_Z and K_Z (C_Z). The y-axis represents the latitude circles (ϕ) where temperature and vertical velocity ω (vertical arrows) decrease with increasing latitude, and the x-axis represents the longitude (λ).

the same interpretation.

The second component of the C_A term contains $(\omega)_\lambda (T)_\lambda \frac{\partial([T]_\lambda)_\varphi}{\partial p}$. Just like the first component, for this one to contribute positively to C_A, it needs to be negative. First, we shall look at the term $\frac{\partial([T]_\lambda)_\varphi}{\partial p}$, which represents the zonal average of the atmospheric lapse rate. Over the cold air mass (between ϕ_3 and ϕ_6, and λ_1 λ_3) this term tends to be negative (temperature increases with height), but only in the lower troposphere, as for the levels above the temperature inversion, the temperature tends to decrease with height. Also, this term tends to be positive in the rest of the domain, especially in the rear of the warm front, for all tropospheric levels. Thus, when averaged across the domain and integrated in vertical levels, this term's contribution tends to be positive. Furthermore, in the rear of the cold front $(\omega)_\lambda$ is positive (descending) and $(T)_\lambda$ is negative (cooler), while in the rear of the warm front $(\omega)_\lambda$ is negative (ascending) and $(T)_\lambda$ is positive (warmer). Therefore, in the case described, $-(\omega)_\lambda (T)_\lambda$ contributes positively to C_A.

From the analysis above, we can see how an extratropical cyclone can modify the global

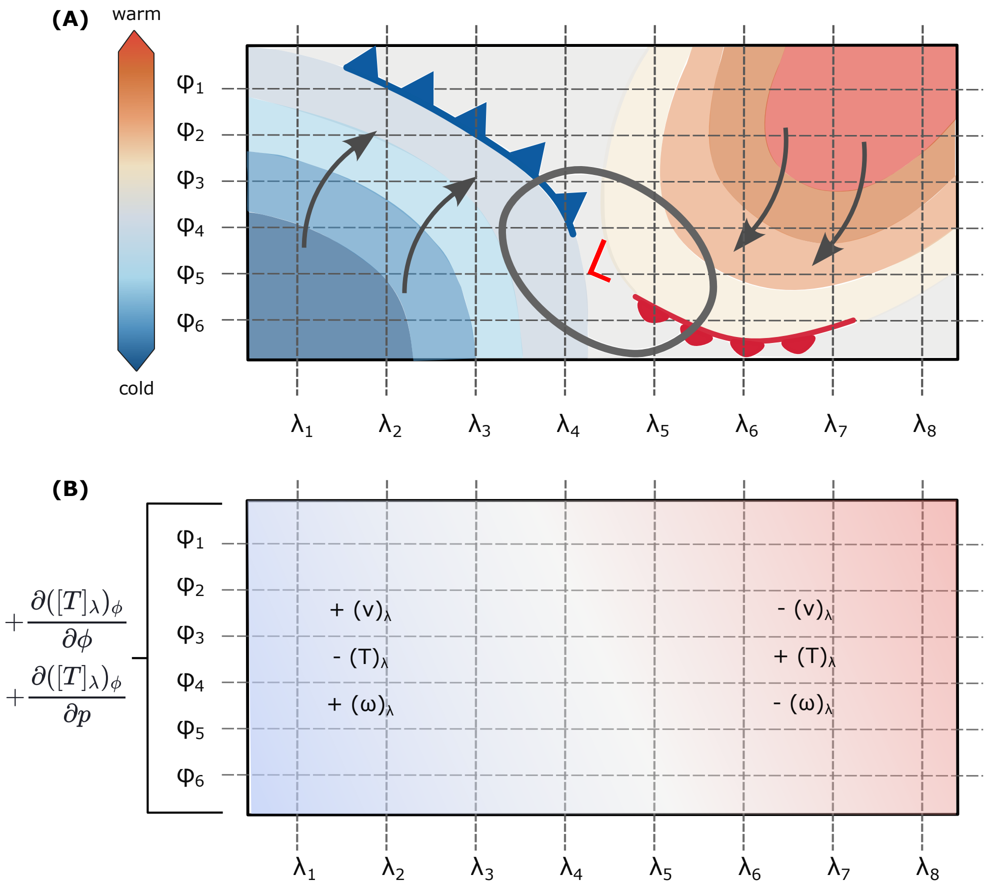

Figure 2.23: Representation of the process of conversion between A_Z to A_E. A) Illustration of an idealized situation of a midlatitude low-pressure system in the Southern Hemisphere, with a cold front propagating west and a warm front east, B) Signal analysis of the variables contained in the formula for C_A (Equation 2.39). The y-axis represents the latitude circles (ϕ) and the x-axis represents the longitude (λ). For the Southern Hemisphere, latitude values decreases from ϕ_1 to ϕ_6.

energetics. Integrating this analysis with the interpretation of the terms A_Z and A_E, it can be seen that C_A acts by transforming the meridional temperature gradients - contained in the formulation for A_Z - into zonal temperature gradients - contained in the formulation for A_E. By doing so, zonal APE is converted into eddy APE. Of course, the scenarios described above are generalizations and do not represent the entirety of the atmospheric profile during the passage of frontal systems. For instance, during the passage of a cold front, $\frac{\partial([T]_\lambda)_\varphi}{\partial p}$ is not positive along all tropospheric levels. However, it is not an understatement to say that the changes described do occur at the lower levels of the atmosphere, and thus we can say that the cold front contribution to the atmosphere energetics is in fact in agreement with the described analysis. Also, both the first and second C_A term don't need to agree in sign: the negative term just needs to be higher in module than the other for C_A to be positive.

The last conversion term, C_K (Equation 2.40, represents the conversion between kinetic energy from the eddies to the zonal mean state. Positive values indicate energy transfer from K_E to K_Z and vice-versa. This term formulation is relatively more complex as from the others, being divided in five distinct terms: 1) meridional advection of zonal momentum, 2) meridional shear of meridional wind, 3) interaction of eddy zonal wind with zonal meridional wind, 4) vertical advection of zonal momentum, 5) vertical advection of meridional momentum

For simplicity, in the first term — the meridional advection of zonal momentum — we shall look at $(u)_\lambda$, $(v)_\lambda$, and $\frac{\partial [u]_\lambda}{\partial \phi}$, as the other variables are related to the transformation from Cartesian to spherical coordinates. To interpret this term, we can analyze a situation where there is a purely zonal westerly jet (Figure 2.24a). In this situation, as the latitude decreases from ϕ_1 to $\phi_1 0$, $\frac{\partial [u]_\lambda}{\partial \phi}$ is negative in the northern part of the domain (between ϕ_1 and ϕ_5) and positive in the southern part (between ϕ_6 and ϕ_{10}). However, v, and therefore $(v)_\lambda$, as well as $(u)_\lambda$, are null. Meanwhile, for a purely meridional northerly jet (Figure 2.24b), $(v)_\lambda$ is negative (more southward) in the jet's core, neutral somewhere between the jet's core and the domain limits, and positive (less southward) near the domain limits. However, $(u)_\lambda$ and $\frac{\partial [u]_\lambda}{\partial \phi}$ are null. Therefore, when averaged through the whole domain, this term is null for both scenarios described.

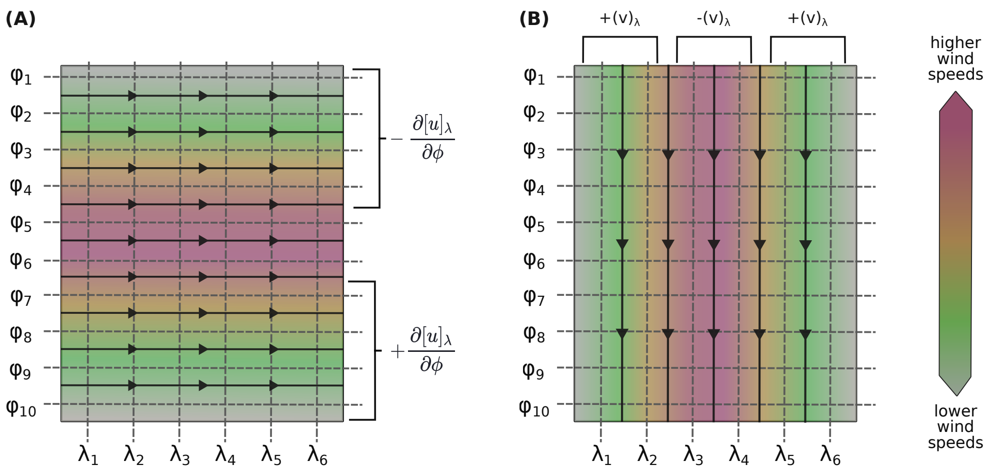

Figure 2.24: Illustration of (A) a zonal westerly jet and (B) a meridional northerly jet in the Southern Hemisphere. The y-axis represents the latitude circles (ϕ) and the x-axis represents the longitude (λ).

We can see that for purely zonal and meridional jets, the first C_K term is null and therefore does not contribute to its signal. However, shall small instabilities in the zonal or meridional flow arise, they may trigger the development of larger instabilities. For instance, we shall look to the situation in the zonal jet where the flow become unstable such there is an cyclonic (clockwise) deviation in the flow at the southern part of the domain (Figure 2.25a). As for the case of the purely meridional jet, $\frac{\partial[u]_\lambda}{\partial\phi}$ is negative for the northern part of the domain and positive for the southern part (Figure 2.25b). However, as the instability arises, $(v)_\lambda$ and $(u)_\lambda$ are no longer null across the whole domain: on the eastern flank of the perturbation they are both negative, while in the western flank they are positive. Altogether, from the signal analysis we can see that $(u)_\lambda\ (v)_\lambda\ \frac{\partial[u]_\lambda}{\partial\phi} > 0$, thus this term contribution for C_K is positive. This means that the eddy, considering only first C_K term alone, is providing energy to the zonal flow and thus loses energy over time and decay.

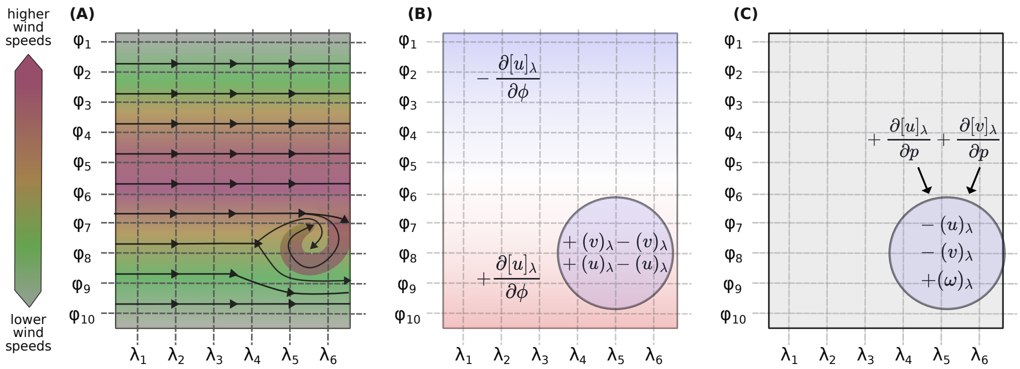

Figure 2.25: A) Illustration of an eddy growing in the northern part of a purely meridional jet, B) signal analysis for the first and C) fourth term of C_K (Equation 2.40), for this situation. The y-axis represents the latitude circles (ϕ) and the x-axis represents the longitude (λ).

The second term in C_K - meridional shear of meridional wind - contains $(v)^2_\lambda \frac{\partial[v]_\lambda}{\partial\phi}$. It is apparent that $(v)^2_\lambda$ is null for purely zonal jets, but otherwise is always positive and thus $\frac{\partial[v]_\lambda}{\partial\phi}$ that will dictate its term contribution to the signal of C_K. Although $\frac{\partial[v]_\lambda}{\partial\phi}$ is always null for purely zonal and meridional jets, it is possible to understand this terms contribution for small instabilities on the zonal flow. For the eddy development illustrated in Figure 2.25a, as $|v|$ decreases from the western to the eastern flank of the perturbation, $[u] < 0$ and thus, in the eddy region $\frac{\partial[v]_\lambda}{\partial\phi} > 0$. Therefore this term's contribution to C_K is positive.

The third term - interaction of eddy zonal wind with zonal meridional wind - contains $(u)^2_\lambda[v]_\lambda$. Both $(u)^2_\lambda$ and $[v]_\lambda$ are null for purely zonal jets, but similarly to the previous terms, we can investigate their combined signal for perturbations in the zonal flow. As

$(u)^2_\lambda$ is always positive, this terms signal is modulated by $[v]_\lambda$. In the case illustrated in Figure 2.25a, as described above, $[v]_\lambda < 0$ and therefore this term's contribution for C_K is negative.

For the fourth and fifth terms - vertical advection of zonal and meridional momentum, respectively - the analysis are more complex due to the tri-dimensional variations in wind wild through the troposphere. the fourth term contains $(\omega)_\lambda (u)_\lambda \frac{\partial [u]_\lambda}{\partial p}$, while the fifth, $(\omega)_\lambda (v)_\lambda \frac{\partial [v]_\lambda}{\partial p}$. In the case of the purely zonal jet both terms are null, but, again, we can investigate their combined signal for perturbations in the zonal flow.

Firstly, for the mid-latitudes we can assume that $\frac{\partial [u]_\lambda}{\partial p}$ is often ($[u]$ increases with height) in the troposphere. However, in the scenario illustrated in Figure 2.25a, assuming the flow is more intense in the eastern than in the western flank of the perturbation, we see that in the perturbation region, $[u]_\lambda$ becomes negative, (westward), thus $\frac{\partial [u]_\lambda}{\partial p} > 0$ (Figure 2.25c). Also, in this case when averaging $(u)_\lambda$ over the domain, the $(u)_\lambda$ from the clockwise deviation in the zonal flow becomes more apparent. Furthermore, if the jet is in altitude (e.g. 250 hPa), the convergence caused by the perturbation results in descending air, i.e., $(\omega)_\lambda$ is positive. Under these specific conditions, this term contribution for C_K is negative. The analysis for the fifth is somewhat similar as for the fourth. Making the same assumptions as before, we have the following: $\frac{\partial [v]_\lambda}{\partial p} > 0$, $(u)_\lambda > 0$ and $(\omega)_\lambda > 0$ (Figure 2.25c). Thus, for the situation illustrated in Figure 2.25a, this term's contribution for C_K is negative.

Altogether, we have the first two terms with positive contributions for C_K signal, while the last three terms have negative contributions. Therefore, the terms that when summed present the highest magnitude that will dictate the signal for C_K. It is important to regard that the illustrative examples provided - zonal and meridional flows and a pertubation growing in the zonal flow - are oversimplifications of atmospheric motion. With them the author do not intend to provide a full picture of the whole set of conditions where conversion between K_Z and K_E might occur. Instead, they serve for guiding thought experiments and can be helpful for understanding this conversion in real atmospheric motions. For the author knowledge, due to the difficulty in making such analysis, no such attempt has been made previously in the literature.

The APE generation and K dissipation terms are defined as:

$$G_Z = \int_{p_t}^{p_b} \frac{[([q]_\lambda)_\phi([T]_\lambda)_\phi]_{\lambda\phi}}{c_p[\sigma]_{\lambda\phi}} dp \tag{2.41}$$

$$G_E = \int_{p_t}^{p_b} \frac{[(q)_\lambda(T)_\lambda]_{\lambda\phi}}{c_p[\sigma]_{\lambda\phi}} dp \tag{2.42}$$

$$D_Z = -\int_{p_t}^{p_b} \frac{1}{g}[[u]_\lambda[F_\lambda]_\lambda + [v]_\lambda[F_\phi]_\lambda]_{\lambda\phi} dp \tag{2.43}$$

$$D_E = -\int_{p_t}^{p_b} \frac{1}{g}[(u)_\lambda(F_\lambda)_\lambda + (v)_\lambda(F_\phi)_\lambda]_{\lambda\phi} dp \tag{2.44}$$

Here, F_λ and F_ϕ represent the zonal and meridional friction components, respectively, and q is the diabatic heating term, computed as a residual from the quasi-geostrophic thermodynamic equation:

$$\frac{q}{c_p} = \frac{\partial T}{\partial t} + \vec{V}_H \cdot \vec{\nabla}_p T - S_p \omega \tag{2.45}$$

where $\vec{V}_H \cdot \vec{\nabla}_p T$ represents the horizontal advection of temperature and S_p approximates the static stability, given by:

$$S_p \equiv -\frac{T}{\theta}\frac{\partial \theta}{\partial p} \tag{2.46}$$

where θ is the potential temperature.

The boundary terms are given by:

$$
\begin{aligned}
\mathrm{BAZ} = {} & c_1 \int_{p_1}^{p_2} \int_{\varphi_1}^{\varphi_2} \frac{1}{2[\sigma]_{\lambda_\varphi}} \left(2\left([T]_\lambda\right)_\varphi (T)_\lambda u + \left([T]_{\lambda_\varphi}\right)_\varphi^2 u \right)_{\lambda_1}^{\lambda_2} \\
& \times d\varphi dp + c_2 \int_{p_1}^{p_2} \frac{1}{2[\sigma]_{\lambda\varphi}} \left(2\left[(v)_\lambda (T)_\lambda\right]_\lambda \left([T]_\lambda\right)_\varphi \cos\varphi \; + \left([T]_\lambda\right)_\varphi^2 [v]_\lambda \cos\varphi \right)_{\varphi_1}^{\varphi_2} dp \\
& - \frac{1}{2[\sigma]_{\lambda\varphi}} \left(\left[2(\omega)_\lambda (T)_\lambda\right]_\lambda \left([T]_\lambda\right)_\varphi + \left[[\omega]_\lambda \left([T]_\lambda\right)_\varphi^2 \right]_{\lambda_\varphi} \right)_{p_1}^{p_2}
\end{aligned}
\tag{2.47}
$$

$$
\begin{aligned}
\mathrm{BAE} = {} & c_1 \int_{p_1}^{p_2} \int_{\varphi_1}^{\varphi_2} \frac{1}{2[\sigma]_{\lambda\varphi}} \left[u (T)_\lambda^2 \right]_{\lambda_1}^{\lambda_2} d\varphi dp \\
& + c_2 \int_{p_1}^{p_2} \frac{1}{2[\sigma]_{\lambda\varphi}} \left(\left[(T)_\lambda^2 v \right]_\lambda \cos\varphi \right)_{\varphi_1}^{\varphi_2} dp \\
& - \left(\frac{[\omega (T)_\lambda^2]_{\lambda\varphi}}{2[\sigma]_{\lambda\varphi}} \right)_{p_1}^{p_2}
\end{aligned}
\tag{2.48}
$$

$$
\begin{aligned}
\mathrm{BKZ} = {} & c_1 \int_{p_1}^{p_2} \int_{\varphi_1}^{\varphi_2} \frac{1}{2g} \left(u \left[u^2 + v^2 - (u)_\lambda^2 - (v)_\lambda^2 \right] \right)_{\lambda_1}^{\lambda_2} \\
& \times d\varphi dp + c_2 \int_{p_1}^{p_2} \frac{1}{2g} \left(\left[v \cos\varphi \left[u^2 + v^2 \;\; - (u)_\lambda^2 - (v)_\lambda^2 \right] \right]_{\varphi_1}^{\varphi_2} dp \right. \\
& - \left(\frac{1}{2g} \left[\omega \left[u^2 + v^2 - (u)_\lambda^2 - (v)_\lambda^2 \right] \right]_{\lambda\varphi} \right)_{p_1}^{p_2}
\end{aligned}
\tag{2.49}
$$

$$
\begin{aligned}
\mathrm{BKE} = {} & c_1 \int_{p_1}^{p_2} \int_{\varphi_1}^{\varphi_2} \frac{1}{2g} \left(u \left[(u)_\lambda^2 + (v)_\lambda^2 \right] \right)_{\lambda_1}^{\lambda_2} d\varphi dp \\
& + c_2 \int_{p_1}^{p_2} \frac{1}{2g} \left(\left[v \cos\varphi \left[(u)_\lambda^2 + (v)_\lambda^2 \right] \right]_\lambda \right)_{\varphi_1}^{\varphi_2} dp \\
& - \left(\frac{1}{2g} \left[\omega \left[(u)_\lambda^2 + (v)_\lambda^2 \right] \right]_{\lambda\varphi} \right)_{p_1}^{p_2}
\end{aligned}
\tag{2.50}
$$

where $c_1 = -\left[a \left(\lambda_2 - \lambda_1 \right) \left(\sin\varphi_2 - \sin\varphi_1 \right) \right]^{-1}, c_2 = -[a \;\; x \left(\sin\varphi_2 - \sin\varphi_1 \right)]^{-1}$.

Lastly, the terms $B\Phi Z$ and $B\Phi E$ are given by:

$$
\begin{aligned}
\mathrm{B\Phi Z} =& c_1 \int_{p_1}^{p_2} \int_{\varphi_1}^{\varphi_2} \frac{1}{g} \left([v]_\lambda \left([\Phi]_\lambda \right)_\varphi \right)_{\lambda_1}^{\lambda_2} d\varphi dp \\
&+ c_2 \int_{p_1}^{p_2} \frac{1}{g} \left(\cos\varphi [v]_\lambda \left([\Phi]_\lambda \right)_\varphi \right)_{\varphi_1}^{\varphi_2} dp \\
&- \frac{1}{g} \left(\left[\left([\omega]_\lambda \right)_\varphi \left([\Phi]_\lambda \right)_\varphi \right]_{\lambda_\varphi} \right)_{p_1}^{p_2}
\end{aligned}
\tag{2.51}
$$

$$
\begin{aligned}
\mathrm{B\Phi E} =& c_1 \int_{p_1}^{p_2} \int_{\varphi_1}^{\varphi_2} \frac{1}{g} \left((u)_\lambda (\Phi)_{\lambda_\lambda} \right)_{\lambda_1}^{\lambda_2} d\varphi dp \\
&+ c_2 \int_{p_1}^{p_2} \frac{1}{g} \left([(v)_\lambda (\Phi)_{\lambda_\lambda}]_\lambda \cos\varphi \right)_{\varphi_1}^{\varphi_2} dp \\
&- \frac{1}{g} \left([(\omega)_\lambda (\Phi)_\lambda]_{\lambda_\varphi} \right)_{p_1}^{p_2}
\end{aligned}
\tag{2.52}
$$

2.4.3 *Lorenz Energy Cycle applied to cyclonic systems*

- Mostrar exemplos de estudos que empregam o LEC para ciclones e os resultados obtidos, e.g.: Veiga et al. (2008); Dias Pinto and Rocha (2011); Michaelides (1987); Michaelides et al. (1999); Muench (1965); Brennan and Vincent (1980).

- Ao final, oferecer uma síntese dos resultados obtidos, já indicando possíveis padrões possíveis na energética de ciclones

Chapter 3

Métodos

3.1 *Fluxograma de atividades*

- Fluxograma demonstrando os passos metodológicos e como se encaixam em cada pergunta de pesquisa

3.2 *Bases de dados utilizadas*

- ERA5
- Tracks do Atlântico Sul (base de dados da Carolina)
- CHIRPS
- QUICKSCAT
- OISST

3.3 *Cálculo do ciclo energético*

- Programa de calculo do LEC (Github) e procedimentos adotados para os cálculos

3.4 *Determinação dos padrões energéticos*

- Padronização da duração dos sistemas através do ciclo de vida
  - Cyclophaser
- Diagrama de fase (Lorenz Phase Space)

- Cálculo da PCA dos termos
- Método K-means

3.5 Descrição do MPAS-A

- Visão geral do modelo
- Descrição do núcleo dinâmico e discretizações numéricas
- Malha adotada e estrutura de grade (horizontal e vertical)
- Opções disponíveis de parametrizações físicas

3.6 Desenho experimental das simulações

3.6.1 Testes de sensibilidade: Furacão Catarina

- Desenho dos experimentos
  - Combinações de parametrizações físicas e de cumulus
  - Duração de cada set de experimentos (3 períodos de 48h cada)
- Inicialização do modelo
- Estrutura de grade adotada (horizontal e vertical)

3.6.2 Experimentos com SST

- Casos escolhidos
- Pertubações adotadas

Chapter 4

Life cycle of cyclones in South America

Chapter 5

Southwestern Atlantic Cyclones Energetics

- Aqui, estou na dúvida se não seria bom criar um capítulo (ou uma seção?) para falar do ciclo de vida dos ciclones, visto que os sistemas serão normalizados a partir disso, havendo diferentes configurações de ciclos de vidas, por exemplo.
- No caso, pensei em criar um capítulo para o ciclo de vida, apresentando os mapas espaciais de modo a indicar que a metodologia utilizada é válida e corresponde ao esperado pela literatura de climatologia de ciclones (ao mesmo tempo em que adiciona novas informações). Entretanto poderia acabar ficando desconexo com os objetivos da tese.
- A alternativa seria apenas incluir como uma seção neste capítulo aqui, de modo que eu indique apenas as configurações de ciclones detectadas pelo programa e mostre alguns exemplos para aferir confiabilidade aos resultados, mas poderia acabar ficando desconexa das outras seções.

5.1 Características gerais

- Estatísticas gerais da energética dos sistemas
- Compósitos para alguns termos, para diferentes fases do ciclo de vida
- Mostrar diagrama de fase para todos os casos

5.2 Padrões energéticos

- Resultados das componentes principais

- Clusters identificados pelo K-means
- Resultados dos padrões energéticos

5.3 Limitações, aplicações e passos futuros

- Limitações: metodologia semi-lagrangiana deve ser interpretada como snapshots (relacionando com Muench (1965))
- A formulação adotada apenas permite a seguinte interpreteção: contribuição para energética global e não a energética individual de cada sistema
- Contextualizar a energética como ferramenta para determinação objetiva das causas eficientes e finais dos ciclones (diagramas do Hart estão relacionados com causas formais e materiais - os trabalhos complementam-se)
- Estudos de caso? (e.g. ciclones extratropicais clássicos formados no sul da ARG, ciclones bomba formados em LA-PLATA, ciclones subtropicais formados em SE-BR e, ciclones tropicais Anita, Iba, 01Q.

Chapter 6

Modelagem numérica

6.1 Testes de sensibilidade: estudo de caso com Furacão Catarina

- Objetivos: 1) determinar qual conjunto de parametrizações de microfísica e cumulus apresentam os melhroes resultados para o Catarina 2) determinar o impacto de diferentes escolhas na energética dos sistemas

6.1.1 Comparação da pressão mínima em superfície e posição do sistema

6.1.2 Precipitação acumulada

6.1.3 Ventos em superfície

6.1.4 Energética

6.2 Experimentos com pertubações no campo de SST

6.2.1 Interação oceano-atmosfera

6.2.2 Ciclo energético

Chapter 7

Conclusões

Conclusões do trabalho e/ou perspectivas

Bibliography

American Meteorological Society, 2012 Cyclone `https://glossary.ametsoc.org/wiki/Cyclone`

Aristotle A., Aristotle Metaphysics. vol. 1, Harvard University Press Cambridge, MA, 1933

Azad R., Sorteberg A., The vorticity budgets of North Atlantic winter extratropical cyclone life cycles in MERRA reanalysis. Part I: Development phase, Journal of the Atmospheric Sciences, 2014a, vol. 71, p. 3109

Azad R., Sorteberg A., The vorticity budgets of North Atlantic winter extratropical cyclone life cycles in MERRA reanalysis. Part II: Decaying phase, Journal of the Atmospheric Sciences, 2014b, vol. 71, p. 3129

Bembenek E., Merlis T. M., Straub D. N., Influence of latitude and moisture effects on the barotropic instability of an idealized ITCZ, Journal of the Atmospheric Sciences, 2021, vol. 78, p. 2677

Bengtsson L., Hodges K. I., Keenlyside N., Will extratropical storms intensify in a warmer climate?, Journal of Climate, 2009, vol. 22, p. 2276

Bjerknes J., On the structure of moving cyclones, Monthly Weather Review, 1919, vol. 47, p. 95

Bjerknes J., Holmboe J., On the theory of cyclones, Journal of Atmospheric Sciences, 1944, vol. 1, p. 1

Bjerknes J., Solberg H., Life cycle of cyclones and the polar front theory of atmospheric circulation. Grondahl, 1922

Bluestein H. B., Synoptic-dynamic Meteorology in Midlatitudes: Observations and theory of weather systems. vol. 2, Taylor & Francis, 1992

Booth J. F., Naud C. M., Jeyaratnam J., Extratropical cyclone precipitation life cycles: A satellite-based analysis, Geophysical Research Letters, 2018, vol. 45, p. 8647

Brennan F. E., Vincent D. G., Zonal and eddy components of the synoptic-scale energy budget during intensification of hurricane Carmen (1974), Monthly Weather Review, 1980, vol. 108, p. 954

Brown Jr J. A., A diagnostic study of tropospheric diabatic heating and the generation of available potential energy, Tellus, 1964, vol. 16, p. 371

Burpee R. W., The origin and structure of easterly waves in the lower troposphere of North Africa, Journal of the Atmospheric Sciences, 1972, vol. 29, p. 77

Cao X., Huang P., Chen G., Chen W., Modulation of western North Pacific tropical cyclone genesis by intraseasonal oscillation of the ITCZ: A statistical analysis, Advances in Atmospheric Sciences, 2012, vol. 29, p. 744

Cardoso A. A., da Rocha R. P., Crespo N. M., Synoptic Climatology of Subtropical Cyclone Impacts on Near-Surface Winds Over the South Atlantic Basin, Earth and Space Science, 2022, vol. 9, p. e2022EA002482

Chan J. C., Kepert J. D., Global perspectives on tropical cyclones: from science to mitigation, 2010

Chang E. K., Lee S., Swanson K. L., Storm track dynamics, Journal of climate, 2002, vol. 15, p. 2163

Charney J. G., The dynamics of long waves in a baroclinic westerly current, Journal of the Atmospheric Sciences, 1947, vol. 4, p. 136

Charney J. G., Eliassen A., On the growth of the hurricane depression, Journal of the Atmospheric Sciences, 1964, vol. 21, p. 68

Craig G. C., Gray S. L., CISK or WISHE as the mechanism for tropical cyclone intensification, Journal of Atmospheric Sciences, 1996, vol. 53, p. 3528

Crespo N. M., da Rocha R. P., Sprenger M., Wernli H., A potential vorticity perspective on cyclogenesis over centre-eastern South America, International Journal of Climatology, 2021, vol. 41, p. 663

Crespo N. M., Reboita M. S., Gozzo L. F., de Jesus E. M., Torres-Alavez J. A., Lagos-Zúñiga M. Á., Torrez-Rodriguez L., Reale M., da Rocha R. P., Assessment of the RegCM4-CORDEX-CORE performance in simulating cyclones affecting the western coast of South America, Climate Dynamics, 2023, vol. 60, p. 2041

da Rocha R. P., Reboita M. S., Gozzo L. F., Dutra L. M. M., de Jesus E. M., Subtropical cyclones over the oceanic basins: a review, Annals of the New York Academy of Sciences, 2019, vol. 1436, p. 138

da Silva Dias P. L., da Silva Dias M. A. F., Seluchi M., de Assis Diniz F., O ciclone Catarina: Análise preliminar da estrutura, dinâmica e previsibilidade. In CONGRESSO BRASILEIRO DE METEOROLOGIA , 2004

Dacre H. F., Gray S. L., The spatial distribution and evolution characteristics of North Atlantic cyclones, Monthly Weather Review, 2009, vol. 137, p. 99

de Souza D., da Silva R. R., Ocean-Land Atmosphere Model (OLAM) performance for major extreme meteorological events near the coastal region of southern Brazil, Climate Research, 2021, vol. 84, p. 1

de Souza D. C., Ramos da Silva R., Gomes da Silva P., Fetter Filho A. F. H., Mendez F. J., Werth D., A hybrid regional climate downscaling for the southern Brazil coastal region, International Journal of Climatology, 2022, vol. 42, p. 6753

Deveson A., Browning K., Hewson T., A classification of FASTEX cyclones using a height-attributable quasi-geostrophic vertical-motion diagnostic, Quarterly Journal of the Royal Meteorological Society: A journal of the atmospheric sciences, applied meteorology and physical oceanography, 2002, vol. 128, p. 93

Dias Pinto J. R., Rocha R. P., The energy cycle and structural evolution of cyclones over southeastern South America in three case studies, Journal of Geophysical Research: Atmospheres, 2011, vol. 116

Donald Ahrens C., Henson R., Meteorology Today: An introduction to weather, climate and the environment. Brooks/Cole, 2015

Dutton J. A., Johnson D. R., The theory of available potential energy and a variational approach to atmospheric energetics, Advances in geophysics, 1967, vol. 12, p. 333

Eady E. T., Long waves and cyclone waves, Tellus, 1949, vol. 1, p. 33

Edmon H. J., Vincent D. G., Large-scale atmospheric conditions during the intensification of Hurricane Carmen (1974) II. Diabatic heating rates and energy budgets, Monthly Weather Review, 1979, vol. 107, p. 295

Emanuel K. A., An air-sea interaction theory for tropical cyclones. Part I: Steady-state maintenance, Journal of Atmospheric Sciences, 1986, vol. 43, p. 585

Emanuel K. A., The dependence of hurricane intensity on climate, Nature, 1987, vol. 326, p. 483

Emanuel K. A., Rotunno R., Polar lows as arctic hurricanes, Tellus A: Dynamic Meteorology and Oceanography, 1989, vol. 41, p. 1

Evans J. L., Hart R. E., Objective indicators of the life cycle evolution of extratropical transition for Atlantic tropical cyclones, Monthly Weather Review, 2003, vol. 131, p. 909

Ferreira R. N., Schubert W. H., Barotropic aspects of ITCZ breakdown, Journal of the Atmospheric Sciences, 1997, vol. 54, p. 261

Frank N. L., Atlantic tropical systems of 1969, Monthly Weather Review, 1970, vol. 98, p. 307

Frank W. M., The structure and energetics of the tropical cyclone I. Storm structure, Monthly Weather Review, 1977a, vol. 105, p. 1119

Frank W. M., The structure and energetics of the tropical cyclone II. Dynamics and energetics, Monthly Weather Review, 1977b, vol. 105, p. 1136

Gall R., The effects of released latent heat in growing baroclinic waves, Journal of the Atmospheric Sciences, 1976, vol. 33, p. 1686

Gan M. A., Rao V. B., Surface cyclogenesis over south America, Monthly Weather Review, 1991, vol. 119, p. 1293

Gan M. A., Rao V. B., The influence of the Andes Cordillera on transient disturbances, Monthly Weather Review, 1994, vol. 122, p. 1141

Gozzo L., Da Rocha R., Gimeno L., Drumond A., Climatology and numerical case study of moisture sources associated with subtropical cyclogenesis over the southwestern Atlantic Ocean, Journal of Geophysical Research: Atmospheres, 2017, vol. 122, p. 5636

Gozzo L. F., da Rocha R. P., Reboita M. S., Sugahara S., Subtropical cyclones over the southwestern South Atlantic: Climatological aspects and case study, Journal of Climate, 2014, vol. 27, p. 8543

Gramcianinov C., Campos R., Soares C. G., de Camargo R., Extreme waves generated by cyclonic winds in the western portion of the South Atlantic Ocean, Ocean Engineering, 2020, vol. 213, p. 107745

Gramcianinov C., Hodges K., Camargo R. d., The properties and genesis environments of South Atlantic cyclones, Climate Dynamics, 2019, vol. 53, p. 4115

Gray S. L., Dacre H. F., Classifying dynamical forcing mechanisms using a climatology of extratropical cyclones, Quarterly Journal of the Royal Meteorological Society: A journal of the atmospheric sciences, applied meteorology and physical oceanography, 2006, vol. 132, p. 1119

Gray W. M., Global view of the origin of tropical disturbances and storms, Monthly Weather Review, 1968, vol. 96, p. 669

Gray W. M., The formation of tropical cyclones, Meteorology and atmospheric physics, 1998, vol. 67, p. 37

Grise K. M., Son S.-W., Gyakum J. R., Intraseasonal and interannual variability in North American storm tracks and its relationship to equatorial Pacific variability, Monthly Weather Review, 2013, vol. 141, p. 3610

Gutowski W. J., Branscome L. E., Stewart D. A., Life cycles of moist baroclinic eddies, Journal of the atmospheric sciences, 1992, vol. 49, p. 306

Hadley G., VI. Concerning the cause of the general trade-winds, Philosophical Transactions of the Royal Society of London, 1735, vol. 39, p. 58

Harrold T., Browning K., The polar low as a baroclinic disturbance, Quarterly Journal of the Royal Meteorological Society, 1969, vol. 95, p. 710

Hart R. E., A cyclone phase space derived from thermal wind and thermal asymmetry, Monthly weather review, 2003, vol. 131, p. 585

Held I. M., The macroturbulence of the troposphere, Tellus A, 1999, vol. 51, p. 59

Holopainen E. O., Investigation of friction and diabatic processes in the atmosphere. vol. 29, na, 1964

Holton J. R., An introduction to dynamic meteorology. vol. 41, American Association of Physics Teachers, 1973, 752

Hoskins B. J., Theory of extratropical cyclones. Springer, 1990, 63

Hoskins B. J., Hodges K. I., New perspectives on the Northern Hemisphere winter storm tracks, Journal of the Atmospheric Sciences, 2002, vol. 59, p. 1041

Hoskins B. J., Hodges K. I., A new perspective on Southern Hemisphere storm tracks, Journal of Climate, 2005, vol. 18, p. 4108

Hoskins B. J., Valdes P. J., On the existence of storm-tracks, Journal of Atmospheric Sciences, 1990, vol. 47, p. 1854

Jensen C. E., Energy transformation and vertical flux processes over the northern hemisphere, Journal of Geophysical Research, 1961, vol. 66, p. 1145

Johnson D. R., The available potential energy of storms, Journal of Atmospheric Sciences, 1970, vol. 27, p. 727

Jorgensen D. P., Zipser E. J., LeMone M. A., Vertical motions in intense hurricanes, Journal of the atmospheric sciences, 1985, vol. 42, p. 839

Knutson T. R., McBride J. L., Chan J., Emanuel K., Holland G., Landsea C., Held I., Kossin J. P., Srivastava A., Sugi M., Tropical cyclones and climate change, Nature geoscience, 2010, vol. 3, p. 157

Kuo H.-l., Dynamic instability of two-dimensional nondivergent flow in a barotropic atmosphere, Journal of Atmospheric sciences, 1949, vol. 6, p. 105

Lorenz E., The nature and theory of the general circulation of the atmosphere, World meteorological organization, 1967, vol. 161

Lorenz E. N., Available Potential Energy and the Maintenance of the General Circulation, Tellus, 1955, vol. 7, p. 157

McLennan N., , 1988 Technical report Marine Bombs Program: Phase II. Pacific Weather Centre

McTaggart-Cowan R., Bosart L. F., Davis C. A., Atallah E. H., Gyakum J. R., Emanuel K. A., Analysis of hurricane Catarina (2004), Monthly Weather Review, 2006, vol. 134, p. 3029

Maloney E. D., Hartmann D. L., The Madden–Julian oscillation, barotropic dynamics, and North Pacific tropical cyclone formation. Part I: Observations, Journal of the atmospheric sciences, 2001, vol. 58, p. 2545

Margules M., Uber die Energie der Sturnie, Jahrb. kair-kon Zent, 1903

Marquet P., On the concept of exergy and available enthalpy: Application to atmospheric energetics, Quarterly Journal of the Royal Meteorological Society, 1991, vol. 117, p. 449

Marquet P., The last paper"On the theory of storm"(Zur Sturmtheorie) published by Max Margules in 1906, arXiv preprint arXiv:1704.06128, 2017

Marrafon V. H., Reboita M. S., da Rocha R. P., de Jesus E. M., Classificação dos tipos de ciclones sobre o Oceano Atlântico Sul em projeções com o RegCM4 E MCGs, Revista Brasileira de Climatologia, 2022, vol. 30, p. 1

Mendes D., Souza E. P., Marengo J. A., Mendes M. C., Climatology of extratropical cyclones over the South American–southern oceans sector, Theoretical and applied climatology, 2010, vol. 100, p. 239

Michaelides S. C., Limited area energetics of Genoa cyclogenesis, Monthly Weather Review, 1987, vol. 115, p. 13

Michaelides S. C., Prezerakos N. G., Flocas H. A., Quasi-Lagrangian energetics of an intense Mediterranean cyclone, Quarterly Journal of the Royal Meteorological Society, 1999, vol. 125, p. 139

Molinari J., Knight D., Dickinson M., Vollaro D., Skubis S., Potential vorticity, easterly waves, and eastern Pacific tropical cyclogenesis, Monthly weather review, 1997, vol. 125, p. 2699

Molinari J., Vollaro D., Skubis S., Dickinson M., Origins and mechanisms of eastern Pacific tropical cyclogenesis: A case study, Monthly Weather Review, 2000, vol. 128, p. 125

Montgomery M. T., Persing J., Smith R. K., Putting to rest WISHE-ful misconceptions for tropical cyclone intensification, Journal of Advances in Modeling Earth Systems, 2015, vol. 7, p. 92

Montgomery M. T., Smith R. K., Paradigms for tropical cyclone intensification, Australian Meteorological and Oceanographic Journal, 2014, vol. 64, p. 37

Muench H. S., On the dynamics of the wintertime stratosphere circulation, Journal of Atmospheric Sciences, 1965, vol. 22, p. 349

Nordeng T. E., Rasmussen E. A., A most beautiful polar low. A case study of a polar low development in the Bear Island region, Tellus A, 1992, vol. 44, p. 81

Norquist D. C., Recker E. E., Reed R. J., The energetics of African wave disturbances as observed during phase III of GATE, Monthly Weather Review, 1977, vol. 105, p. 334

Novak L., Tailleux R., On the local view of atmospheric available potential energy, Journal of the Atmospheric Sciences, 2018, vol. 75, p. 1891

Oort A. H., On estimates of the atmospheric energy cycle, Monthly Weather Review, 1964, vol. 92

Ooyama K. V., Conceptual evolution of the theory and modeling of the tropical cyclone, Journal of the Meteorological Society of Japan. Ser. II, 1982, vol. 60, p. 369

Ozawa H., Shimokawa S., Thermodynamics of a tropical cyclone: Generation and dissipation of mechanical energy in a self-driven convection system, Tellus A: Dynamic Meteorology and Oceanography, 2015, vol. 67, p. 24216

Palmén E. H., Newton C. W., Atmospheric circulation systems: their structure and physical interpretation. vol. 13, Academic press, 1969

Pereira Filho A. J., Pezza A. B., Simmonds I., Lima R. S., Vianna M., New perspectives on the synoptic and mesoscale structure of Hurricane Catarina, Atmospheric Research, 2010, vol. 95, p. 157

Petterssen S., Smebye S., On the development of extratropical cyclones, Quarterly Journal of the Royal Meteorological Society, 1971, vol. 97, p. 457

Pezza A. B., Simmonds I., The first South Atlantic hurricane: Unprecedented blocking, low shear and climate change, Geophysical Research Letters, 2005, vol. 32

Pezza A. B., Simmonds I., Pereira Filho A. J., Climate perspective on the large-scale circulation associated with the transition of the first South Atlantic hurricane, International Journal of Climatology: A Journal of the Royal Meteorological Society, 2009, vol. 29, p. 1116

Pinto J. G., Spangehl T., Ulbrich U., Speth P., Sensitivities of a cyclone detection and tracking algorithm: individual tracks and climatology, Meteorologische Zeitschrift, 2005, vol. 14, p. 823

Plumb R. A., A new look at the energy cycle, Journal of Atmospheric Sciences, 1983, vol. 40, p. 1669

Ramage C. S., Hurricane development, Journal of Atmospheric Sciences, 1959, vol. 16, p. 227

Rasmussen E., The polar low as an extratropical CISK disturbance, Quarterly Journal of the Royal Meteorological Society, 1979, vol. 105, p. 531

Rasmussen E., A case study of a polar low development over the Barents Sea, Tellus A, 1985, vol. 37, p. 407

Rasmussen E. A., A comparative study of tropical cyclones and polar lows. vol. 47, A. Deepak Publishing, 1989, 80

Reboita M., Crespo N., Dutra L., Silva B., Capucin B., da Rocha R., Iba: the first pure tropical cyclogenesis over the western South Atlantic Ocean, Journal of Geophysical Research: Atmospheres, 2021, vol. 126, p. e2020JD033431

Reboita M. S., Da Rocha R. P., Ambrizzi T., Sugahara S., South Atlantic Ocean cyclogenesis climatology simulated by regional climate model (RegCM3), Climate Dynamics, 2010, vol. 35, p. 1331

Reboita M. S., Da Rocha R. P., Oliveira D. M. d., Key features and adverse weather of the named subtropical cyclones over the Southwestern South Atlantic Ocean, Atmosphere, 2018, vol. 10, p. 6

Reboita M. S., Gan M. A., Rocha R. P. d., Ambrizzi T., Regimes de precipitação na América do Sul: uma revisão bibliográfica, Revista brasileira de meteorologia, 2010, vol. 25, p. 185

Reboita M. S., Gan M. A., Rocha R. P. d., Custódio I. S., Ciclones em superfície nas latitudes austrais: Parte I-revisão bibliográfica, Revista Brasileira de Meteorologia, 2017, vol. 32, p. 171

Reboita M. S., Gozzo L. F., Crespo N. M., Custodio M. d. S., Lucyrio V., de Jesus E. M., da Rocha R. P., From a Shapiro–Keyser extratropical cyclone to the subtropical cyclone Raoni: An unusual winter synoptic situation over the South Atlantic Ocean, Quarterly Journal of the Royal Meteorological Society, 2022, vol. 148, p. 2991

Reboita M. S., Oliveira D., Da Rocha R., Dutra L., Subtropical cyclone Anita's potential to tropical transition under warmer sea surface temperature scenarios, Geophysical Research Letters, 2019, vol. 46, p. 8484

Reed R. J., Norquist D. C., Recker E. E., The structure and properties of African wave disturbances as observed during phase III of GATE, Monthly Weather Review, 1977, vol. 105, p. 317

Reed R. J., Wolfe J. L., Nishimoto H., A spectral analysis of the energetics of the stratospheric sudden warming of early 1957, Journal of the Atmospheric Sciences, 1963, vol. 20, p. 256

Rennick M. A., The generation of African waves, Journal of Atmospheric Sciences, 1976, vol. 33, p. 1955

Riehl H., On the formation of typhoons, Journal of the Atmospheric Sciences, 1948, vol. 5, p. 247

Robertson F., Smith P., The impact of model moist processes on the energetics of extra-tropical cyclones, Monthly Weather Review, 1983, vol. 111, p. 723

Rudeva I., Gulev S. K., Climatology of cyclone size characteristics and their changes during the cyclone life cycle, Monthly Weather Review, 2007, vol. 135, p. 2568

Saltzman B., Fleisher A., Further statistics on the modes of release of available potential energy, Journal of Geophysical Research, 1961, vol. 66, p. 2271

Schemm S., Sprenger M., Wernli H., When during their life cycle are extratropical cyclones attended by fronts?, Bulletin of the American Meteorological Society, 2018, vol. 99, p. 149

Schneider T., The general circulation of the atmosphere, Annu. Rev. Earth Planet. Sci., 2006, vol. 34, p. 655

Schultz D. M., Keyser D., Bosart L. F., The effect of large-scale flow on low-level frontal structure and evolution in midlatitude cyclones, Monthly weather review, 1998, vol. 126, p. 1767

Shapiro M. A., Keyser D., Fronts, jet streams and the tropopause. Springer, 1990

Shea D. J., Gray W. M., The hurricane's inner core region. I. Symmetric and asymmetric structure, Journal of the Atmospheric Sciences, 1973, vol. 30, p. 1544

Silva Dias P. L., Gan M., Beven J. L., Pezza A., Holland G., Pereira A., McTaggart-Cowan R., Diniz F. d. A., Seluchi M., Braga H. J., The Catarina Phenomenon. In Proceedings of the Sixth International Workshop on Tropical Cyclones , São Paulo, Brazil, 2004

Simmonds I., Size changes over the life of sea level cyclones in the NCEP reanalysis, Monthly Weather Review, 2000, vol. 128, p. 4118

Simmonds I., Keay K., Mean Southern Hemisphere extratropical cyclone behavior in the 40-year NCEP–NCAR reanalysis, Journal of Climate, 2000, vol. 13, p. 873

Simmonds I., Murray R. J., Southern extratropical cyclone behavior in ECMWF analyses during the FROST special observing periods, Weather and forecasting, 1999, vol. 14, p. 878

Simpson R. H., Evolution of the Kona storm a subtropical cyclone, Journal of Atmospheric Sciences, 1952, vol. 9, p. 24

Sinclair M. R., An objective cyclone climatology for the Southern Hemisphere, Monthly Weather Review, 1994, vol. 122, p. 2239

Sinclair M. R., A climatology of cyclogenesis for the Southern Hemisphere, Monthly Weather Review, 1995, vol. 123, p. 1601

Smith P. J., On the contribution of a limited region to the global energy budget, Tellus, 1969, vol. 21, p. 202

Smith P. J., Vincent D. G., Edmond Jr H. J., The time dependence of reference pressure in limited region available potential energy budget equations, Tellus, 1977, vol. 29, p. 476

Spiridonov V., Ćurić M., Fundamentals of meteorology. Springer, 2021

Starr V. P., Note concerning the nature of the large-scale eddies in the atmosphere, Tellus, 1953, vol. 5, p. 494

Starr V. P., Further statistics concerning the general circulation, Tellus, 1959, vol. 11, p. 481

Stoll P. J., Spengler T., Terpstra A., Graversen R. G., Polar lows–moist-baroclinic cyclones developing in four different vertical wind shear environments, Weather and Climate Dynamics, 2021, vol. 2, p. 19

Stull R. B., Practical meteorology: an algebra-based survey of atmospheric science. University of British Columbia, 2015

Sutcliffe R., A contribution to the problem of development, Quarterly Journal of the Royal Meteorological Society, 1947, vol. 73, p. 370

Terry J. P., Tropical cyclones: climatology and impacts in the South Pacific. Springer Science & Business Media, 2007

Tibaldi S., Buzzi A., Malguzzi P., Orographically induced cyclogenesis: Analysis of numerical experiments, Monthly Weather Review, 1980, vol. 108, p. 1302

Trenberth K. E., On the interpretation of the diagnostic quasi-geostrophic omega equation, Mon. Wea. Rev, 1978, vol. 106, p. 131

Trigo I. F., Climatology and interannual variability of storm-tracks in the Euro-Atlantic sector: a comparison between ERA-40 and NCEP/NCAR reanalyses, Climate Dynamics, 2006, vol. 26, p. 127

Veiga J. A. P., Pezza A. B., Simmonds I., Silva Dias P. L., An analysis of the environmental energetics associated with the transition of the first South Atlantic hurricane, Geophysical Research Letters, 2008, vol. 35

Vera C. S., Vigliarolo P. K., Berbery E. H., Cold season synoptic-scale waves over subtropical South America, Monthly Weather Review, 2002, vol. 130, p. 684

Vianna M., Menezes V., Pezza A., Simmonds I., Interactions between Hurricane Catarina (2004) and warm core rings in the South Atlantic Ocean, Journal of Geophysical Research: Oceans, 2010, vol. 115

Vincent D., Chang L., Some further considerations concerning energy budgets of moving systems, Tellus, 1973, vol. 25, p. 224

Walsh K., Tropical cyclones and climate change: unresolved issues, Climate Research, 2004, vol. 27, p. 77

Walsh K. J., Camargo S. J., Knutson T. R., Kossin J., Lee T.-C., Murakami H., Patricola C., Tropical cyclones and climate change, Tropical Cyclone Research and Review, 2019, vol. 8, p. 240

Walsh K. J., McBride J. L., Klotzbach P. J., Balachandran S., Camargo S. J., Holland G., Knutson T. R., Kossin J. P., Lee T.-c., Sobel A., et al., Tropical cyclones and climate change, Wiley Interdisciplinary Reviews: Climate Change, 2016, vol. 7, p. 65

Wang D., Lin Y., Chavas D. R., Tropical cyclone potential size, Journal of the Atmospheric Sciences, 2022, vol. 79, p. 3001

Weatherford C. L., Gray W. M., Typhoon structure as revealed by aircraft reconnaissance. Part I: Data analysis and climatology, Monthly Weather Review, 1988, vol. 116, p. 1032

Whitaker J. S., Davis C. A., Cyclogenesis in a saturated environment, Journal of the atmospheric sciences, 1994, vol. 51, p. 889

Whittaker L., Horn L., Northern Hemisphere extratropical cyclone activity for four mid-season months, Journal of Climatology, 1984, vol. 4, p. 297

Wiin-Nielsen A., A study of energy conversion and meridional circulation for the large-scale motion in the atmosphere, Monthly Weather Review, 1959, vol. 87, p. 319

Wiin-Nielsen A., Brown J. A., Drake M., On atmospheric energy conversions between the zonal flow and the eddies, Tellus, 1963, vol. 15, p. 261

Willoughby H. E., Marks F. D., Feinberg R. J., Stationary and moving convective bands in hurricanes, Journal of the Atmospheric Sciences, 1984, vol. 41, p. 3189

Wu M.-L. C., Reale O., Schubert S. D., Suarez M. J., Thorncroft C. D., African easterly jet: Barotropic instability, waves, and cyclogenesis, Journal of Climate, 2012, vol. 25, p. 1489

Yanai M., A detailed analysis of typhoon formation, Journal of the Meteorological Society of Japan. Ser. II, 1961, vol. 39, p. 187

Yanase W., Niino H., Hodges K., Kitabatake N., Parameter spaces of environmental fields responsible for cyclone development from tropics to extratropics, Journal of Climate, 2014, vol. 27, p. 652

Yano J.-I., Emanuel K., An improved model of the equatorial troposphere and its coupling with the stratosphere, Journal of Atmospheric Sciences, 1991, vol. 48, p. 377

Zehr R. M., Tropical cyclogenesis in the western North Pacific, 1992

Appendix

Appendix A

título do apêndice 01

A.1 subtítulo 01

Appendix B

título do apêndice 02